IEEE Access
Multidisciplinary : Rapid Review : Open Access Journal

Received June 17, 2020, accepted July 15, 2020, date of publication July 22, 2020, date of current version August 5, 2020.

Digital Object Identifier 10.1109/ACCESS.2020.3011144

Performance Analysis of Rate Splitting in *K*-User Interference Channel Under Imperfect CSIT: Average Sum Rate, Outage Probability and SER

XIN SU, (Member, IEEE), YIFEI YUAN, (Senior Member, IEEE), AND QIXING WANG
Future Mobile Technology Laboratory, China Mobile Research Institute, Beijing 100053, China

Corresponding author: Xin Su (suxin@chinamobile.com)

ABSTRACT Interference alignment (IA) and rate splitting (RS) are two promising interference processing techniques to handle the interference problems in the multi-input multi-output (MIMO) multi-cell cooperation scenario. However, under the imperfect channel state information (CSIT) in the practical systems, the poor robustness of IA has become a bottleneck of its performance gain. On the other hand, RS can provide a robust solution, yet its outage performance is limited by its SIC decoding process. To make up these two schemes' shortcomings and achieve the robust and reliable multi-cell cooperation, in this paper, we propose a novel transmission scheme, signal and interference alignment based rate splitting (SIA-RS), and provide comprehensively analyze the performance under CSIT quantization error. Closed-from expressions are derived for the average sum rate, outage probability and symbol error rate (SER) and their asymptotic versions in high signal-to-noise ratio (SNR) region. Due to signal alignment and common message, there exists certain correlation between the key variables. The nested finite weighted sum of independent and correlated Erlang random variables is used to approximate the exact expressions of performance. The relationship between ''splitting'' and ''alignment'' is revealed via the analytical derivation and numerical simulation. The simulation results show that the proposed SIA-RS achieves the best average sum rate compared with conventional IA and RS schemes, indicate that alignment would further reduce the outage probability, and suggest to the separate modulation schemes for common and private messages in terms of SER.

INDEX TERMS Average sum rate, imperfect CSIT, interference alignment, interference channel, MIMO, outage probability, rate splitting, SER.

I. INTRODUCTION

To satisfy the ever increasing demand of explosive growth of traffic for high date and mobility, the network deployment tends to be more ultra-dense and complicated, resulting in more severe interference. The traditional view is to treat interference as detriment and try to avoid it, which leads to inefficient use of wireless resources. Rethinking the role of interference as useful resources has been the mainstream idea for interference processing [1]. Multi-cell cooperation is just one of the typical examples to explore the potential of utilizing interference, where multiple base stations (BSs) jointly design the transceiver strategies to control the inter-cell interference (ICI) via information sharing.

The associate editor coordinating the review of this manuscript and approving it for publication was Ahmed Farouk.

A. RELATED WORKS

Under the cooperation framework, interference alignment (IA), first proposed by Cadambe and Jafar [2], is degree of freedom (DoF) optimal in interference channel, which means it can achieve the capacity bound under the extremely high signal-to-noise ratio (SNR) scenario. If the channel state information (CSI) is perfectly known, IA enables projecting multiple interference signals onto the smallest possible subspace at each receiver and guarantees the decodability for desired signals by designing the transceivers. Nevertheless, in the practical systems, it is nearly impossible to acquire global, instantaneous and accurate CSI, and thus the high-dependency on ideal CSI is one of the major obstacles for IA to be useful in practical systems [3]. The corresponding performance degradation stems from two reasons. One reason is that the assumption of perfect CSI is too optimistic for IA to be robust. The other one is that the DoF is a too conservative metric, that is, to assumed that interference and desired links have the comparable strength, each carrying one DoF. Hence DoF-optimal IA inherently cannot exploit the interference strength to differentiate weak or strong interference. In that, these interference can usually be sufficiently processed without the accurate CSI.

Rate splitting (RS) is another interference processing technique, first proposed by Han and Kobayashi in 1981. It has been proved that RS can achieve the optimal inner bound of capacity (HK region) for two-user interference channel [4]. The main idea of RS is that each transmitted message is divided into a common part and a private part, and each receiver performs successive interference cancellation (SIC) to decode and remove the common part first before decoding the private part. Different from IA, by considering the interference strength, RS can do the soft switching between two interference processing techniques for two extreme interference conditions, i.e., treating the weak interference as noise and decoding the strong one via adjusting the power allocated to common and private parts. RS has been used as a tool to prove the achievability of capacity region. In [5], RS is proved to achieve the optimal DoF in multiple input single output (MISO) broadcast channel (BC) under imperfect CSI at transmitter (CSIT). Reference [6] claims that RS can obtain the optimal generalized DoF (GDoF) in K-user interference channel under finite precision CSIT. These studies confirm that RS is robust to imperfect CSIT from the perspective of information theory.

In recent years, the RS based transceiver design and implementation have been studied extensively. The basic implementation framework of RS strategy for multi-user multi-input multi-output (MU-MIMO) systems was developed in [7]. Following up on this framework, [8]–[11] study the the feedback overhead, transceiver design and performance gain for RS specific implementations. In [8], the number of feedback bits needed by RS was derived via minimizing the rate loss relative to conventional zero-forcing (ZF) under perfect CSIT, and shows that RS can reduce the feedback overhead over ZF with quantized CSIT. In [9], common and private beamforming and power allocation of RS was optimized by maximizing weighted sum rate for MIMO BC. And the max-min fairness and power minimization problems were solved to optimize the common and private beamforming vectors in [10]. RS was also applied into massive MIMO BC in [11], and a novel hierarchical RS (HRS) is proposed to reduce the dependency on CSIT with transmit correlation matrix.

Notice that there is a similar superposition coding & SIC (SC-SIC) process in the conventional non-orthogonal multiple access (NOMA) over power domain, and RS also involves the conventional space-division multiple access (SDMA) for private messages. So it is necessary to compare NOMA, SDMA and RS multiple access (RSMA), which has been discussed sufficiently in [12]. RSMA is a more general framework of MU transmission, and SDMA and NOMA can be treated as the special cases of RSMA; RSMA is a bridging between SDMA and NOMA, that is, decoding interference partially and treating interference as nois partially; RSMA is more robust than SDMA and NOMA in terms of user deployments (channel direction and strength), CSIT accuracy and network load (over- or under-loaded) and can achieve equal or higher rate than that of SDMA and NOMA; RSMA can deliver better rate and quality of service (QoS) than NOMA, using the transmit scheduling and receiver (the number of SIC layers) with lower complicity.

As mentioned before, the imperfect CSIT has limited the performance gain from multi-cell cooperation techniques, especially for IA. RS can also be applied to multi-cell scenarios to improve the robustness to imperfect CSIT. Compared with the studies in BC systems, there are very limited studies on RS-based multi-cell cooperation strategies. For MISO interference channel, the topological RS is proposed in [13] in terms of DoF metric, under some specific assumptions on imperfect CSIT qualities. Due to the difficulty of solving more complicated topology for more users, an easier implementation of RS for multi-cell cooperation is stated in [14], which is similar to the framework for MU-MIMO given in [7].

B. MOTIVATIONS AND CONTRIBUTIONS

Until now, most studies on RS performance focus on proving DoF or GDoF from the perspective of information theory, and the spectral efficiency (SE) oriented optimization problems from the perspective of algorithm design. There is few analysis of RS performance from the implementation standpoint, with the concerns about the average rate, outage probability and symbol error rate (SER) at an arbitrary SNR, under the time-varying fading channel and under imperfect CSIT. This study tries to provide a guideline for system designs and performance optimization, assessing the impact of the relevant parameters on the performance, such as how to allocate the power between common and private messages.

Moreover, as two information-theory optimal interference processing techniques, IA and RS are usually studied separately. The early work in [15] proposed a scheme combining IA and RS mechanically in a special setting, 3-user interference channel, and without any non-ideal CSIT assumptions. Actually, the ideas of ''splitting'' and ''alignment'' can be combined to compensate each other. IA is very sensitive to imperfect CSIT while RS is robust. The SIC process of RS introduces error propagation and increases the outage probability while [16] and [17] have proved that two aligned superimposed signals over power domain have better chance to be decoded by SIC.

The major contributions of this paper can be summarized as follows.

- We propose a novel signal and interference alignment based RS (SIA-RS) transmission scheme, which combines the robustness from "splitting" and reliability from "alignment". The common and private desired signals are aligned to improve SIC decoding performance, and the private interference signals are mitigated by IA. The common signal of RS has lower dependency on perfect CSIT and can bring out extra multiplexing gain.
- A comprehensive analysis of performance under CSIT quantization error is carried out, leading to the closed-form formulas of average sum rate, outage probability and SER. Because of the signal alignment and common message, the correlation between the key random variables (RVs) is revealed. The nested finite weighted sum of independent and correlated Erlang RVs are used to approximate the exact but tedious expressions.
- The asymptotic performance loss at high SNR is analyzed using the simplified expressions, which provides insight into the relationships between performance trend and some key system parameters.
- Based on the closed-from formulas, the simulation results illustrate that the proposed SIA-RS has the best average sum rate compared with conventional IA and RS schemes, verify that alignment can further improve the outage probability, and enlighten us as to the separate modulation schemes for common and private messages.

The remainder of this paper is organized as follows. Section II starts from the system model of K-User MIMO interference channel and the basic principle of RS transmission, and then proposes SIA-RS strategy considering CSIT quantization error model. In Section III, the derivation processes of average sum rate, outage probability and SER, respectively, along with some necessary preliminaries are elaborated. Next, we derive the asymptotic performance loss relative to the performance under perfect CSIT at high SNR in Section IV. In Section V, the simulation results are presented to validate the theoretical claims. At last, the paper is concluded in Section VI.

Notations: In this paper, scalars are denoted by italic letters. Vectors and matrices are denoted by bold-face letters. Sets are denoted by script upper-case letters, such as $\mathcal{X}$. $\mathbb{C}^{M\times N}$ denotes the space of $M \times N$ complex-valued matrices. For a complex-value vector, $\mathbf{v}$, $\|\mathbf{v}\|$, $\mathbf{v}^{\mathrm{T}}$ and $\mathbf{v}^{\mathrm{H}}$ denote its l_2-norm, transpose, conjugate transpose, respectively. $\otimes$ is Kronecker's product. $\mathcal{X} \times \mathcal{Y}$ denotes the Cartesian product of two sets. span$(\cdot)$ denotes a space spanned by the column vectors of a matrix. $\mathbb{E}\{\cdot\}$ denotes the expectation operators. vec$(\cdot)$ and rvec$(\cdot)$ denote the vectorization operator and its inverse transform, respectively.

II. SYSTEM MODEL

Consider K-user MIMO interference channel, where each transmitter (TX) is equipped with N_t antennas and each receiver (RX) has N_r antennas. Let $\mathcal{K} \triangleq \{1, 2, \ldots, K\}$. TX k directs a message W_k uniformly drawn from the set $\mathcal{W}_k$ to its corresponding receiver, RX k. RS scheme is implemented through splitting each message into a private part and a common part, i.e., $W_k = \{W_k^{(c)}, W_k^{(p)}\}$ with $W_k^{(p)} \in \mathcal{W}_k^{(p)}$, $W_k^{(c)} \in \mathcal{W}_k^{(c)}$ and $\mathcal{W}_k^{(p)} \times \mathcal{W}_k^{(c)} = \mathcal{W}_k$. A super common message is introduced for $\mathcal{K}$, which is obtained by packing the common parts of all the users such that $W^{(c)} = \{W_k^{(c)}\}_{k\in\mathcal{K}}$. it is assumed that private and common messages are independent identically distributed (i.i.d.) encoded into single-layer symbols $s_k^{(p)} \sim \mathcal{CN}(0, 1)$ and $s^{(c)} \sim \mathcal{CN}(0, 1)$, respectively. With superimposition coding, the transmitted signal of TX k can be written as

$$\mathbf{x}_k = \sqrt{tP}\mathbf{v}_k^{(p)}s_k^{(p)} + \sqrt{(1-t)P}\mathbf{v}_k^{(c)}s^{(c)}, \tag{1}$$

where $\mathbf{v}_k^{(p)} \in \mathbb{C}^{N_t\times 1}$ and $\mathbf{v}_k^{(c)} \in \mathbb{C}^{N_t\times 1}$ are the private and common beamforming vectors with unit norm, respectively, i.e., $\|\mathbf{v}_k^{(p)}\|^2 = \|\mathbf{v}_k^{(c)}\|^2 = 1, \forall k \in \mathcal{K}$, P is the maximum transmit power per TX, and $t \in (0, 1]$ is a power allocation factor between common and private parts.

The received signal at RX k is represented as

$$\begin{aligned}\mathbf{y}_k &= \sum_{j\in\mathcal{K}} \mathbf{H}_{k,j}\mathbf{x}_j + \mathbf{n}_k \\ &= \underbrace{\sqrt{tP}\mathbf{H}_{k,k}\mathbf{v}_k^{(p)}s_k^{(p)} + \sqrt{(1-t)P}\mathbf{H}_k\mathbf{v}^{(c)}s^{(c)}}_{\text{Desired signal subspace}} \\ &\quad + \underbrace{\sum_{j\in\mathcal{K}\setminus\{k\}} \sqrt{tP}\mathbf{H}_{k,j}\mathbf{v}_j^{(p)}s_j^{(p)}}_{\text{Interference subspace}} + \mathbf{n}_k,\end{aligned} \tag{2}$$

where $\mathbf{H}_{k,j} \in \mathbb{C}^{N_r\times N_t}$ is the channel matrix from TX j to RX k with i.i.d. zero-mean and unit-variance complex Gaussian entries. Let $\mathbf{H}_k \triangleq [\mathbf{H}_{k,1}, \ldots, \mathbf{H}_{k,K}] \in \mathbb{C}^{N_r\times KN_t}$, and $\mathbf{v}^{(c)} \triangleq [\mathbf{v}_1^{(c)\mathrm{H}}, \ldots, \mathbf{v}_K^{(c)\mathrm{H}}]^{\mathrm{H}} \in \mathbb{C}^{KN_t\times 1}$. $\mathbf{n}_k \sim \mathcal{CN}(0, \sigma_n^2\mathbf{I}_{N_r})$ is the additive white Gaussian noise (AWGN) at RX k.

Then, RX k uses receive filter vector $\mathbf{u}_k \in \mathbb{C}^{N_r\times 1}$ to obtain $\hat{s}_k = \mathbf{u}_k^{\mathrm{H}}\mathbf{y}_k$, where $\|\mathbf{u}_k\|^2 = 1$, $k \in \mathcal{K}$. If each node has a knowledge of the perfect CSIT, the interference from private signals is mitigated via IA, satisfying the following equations,

$$(\mathbf{u}_k)^{\mathrm{H}}\mathbf{H}_{k,j}\mathbf{v}_j^{(p)} = 0, \quad \forall k \neq j,\ \forall k, j \in \mathcal{K}. \tag{3}$$

Finally, based on the power allocation between private and common signals, RX k can employ SIC: first, to decode common part and subtract it from received signal, and then to detect the private part.

A. SIGNAL AND INTERFERENCE ALIGNMENT BASED RATE SPLITTING TRANSMISSION

According to [16], the relatively higher spatial correlation is beneficial to the SIC, which is also evidenced by the improvement of conventional NOMA performance with spatially aligned users. Therefore, besides implementing IA to cancel the ICI from private signals, this paper uses the signal alignment to align the common and private signals in signal subspace. The transmission strategy is called signal and interference alignment based rate splitting (SIA-RS).

First, the channel-independent random beamforming vector, $\mathbf{v}^{(c)}$, is used to transmit the common signals, which satisfies the transmission power constraint $\|\mathbf{v}^{(c)}\|^2 = K$. The common beamforming vector is treated as random alignment reference vector [18].

Next, all the common signals are aligned with private signal space, that is,

$$\text{span}\left(\mathbf{H}_{k,k}\mathbf{v}_k^{(p)}\right) = \text{span}\left(\mathbf{H}_k\mathbf{v}^{(c)}\right). \tag{4}$$

If each node has a knowledge of the perfect CSIT, the signal alignment between common and private parts from TX k is perfect, and thus can be represented as

$$\mathbf{g}_{k,k} = \mathbf{H}_{k,k}\mathbf{v}_k^{(p)} = c_k^{(p)}\mathbf{H}_k\mathbf{v}^{(c)}, \quad \forall k \in \mathcal{K}, \tag{5}$$

where $c_k^{(p)} \in \mathbb{R}^+$ is used to adjust the transmission power to satisfy the constraint. Let $\mathbf{g}_{k,j} \triangleq \mathbf{H}_{k,j}\mathbf{v}_j^{(p)}, \forall k, j \in \mathcal{K}$.

To facilitate analysis, without losing generality, assuming $N_t = N_r = K$ herein, multiplying $\mathbf{H}_{k,k}^{-1}$ to both sides of equation (5), the private beamforming vector is obtained,

$$\mathbf{v}_k^{(p)} = \frac{\mathbf{H}_{k,k}^{-1}\mathbf{H}_k\mathbf{v}^{(c)}}{\left\|\mathbf{H}_{k,k}^{-1}\mathbf{H}_k\mathbf{v}^{(c)}\right\|} = c_k^{(p)}\mathbf{H}_{k,k}^{-1}\mathbf{H}_k\mathbf{v}^{(c)}, \quad \forall k \in \mathcal{K}. \tag{6}$$

Then, RX k decodes the aligned desired signal with reception filter vector $\mathbf{u}_k$,

$$\hat{s}_k = \underbrace{\sqrt{P}\mathbf{u}_k^{\text{H}}\mathbf{H}_{k,k}\mathbf{v}^{(p)}\left(\sqrt{t}s_k^{(p)} + \frac{\sqrt{1-t}}{c_k^{(p)}}s^{(c)}\right)}_{\text{Aligned desired signal subspace}} + \underbrace{\sqrt{tP}\sum_{j\in\mathcal{K}\setminus\{k\}}\mathbf{u}_k^{\text{H}}\mathbf{H}_{k,j}\mathbf{v}_j^{(p)}s_j^{(p)}}_{\text{ICI}} + \mathbf{u}_k^{\text{H}}\mathbf{n}_k. \tag{7}$$

Considering the perfect knowledge of CSIT, the common and private signals can be aligned onto a signal space perfectly and ICI can be canceled based on (3) completely. Accordingly, we have the superposition of private and common signals in power domain, that is,

$$\hat{s}_k = \sqrt{P}h_{k,k}\left(\sqrt{t}s_k^{(p)} + \frac{\sqrt{1-t}}{c_k^{(p)}}s^{(c)}\right) + \mathbf{u}_k^{\text{H}}\mathbf{n}_k, \tag{8}$$

where $h_{k,j} \triangleq \mathbf{u}_k^{\text{H}}\mathbf{H}_{k,j}\mathbf{v}_j^{(p)}, \forall k, j \in \mathcal{K}$; $h_{k,j} = 0$ for $k \neq j$ with perfect IA.

Finally, to adjust the power allocation factor t enables RX k to implement SIC. RX k first decodes common message with signal-to-interference-plus-noise ratio (SINR),

$$\text{SINR}_k^{(c)} = \frac{(1-t)P/(c_k^{(p)})^2|h_{k,k}|^2}{tP|h_{k,k}|^2 + \sigma_n^2}. \tag{9}$$

To ensure the common message be decodable for all the RXs, $W^{(c)}$ is transmitted at the minimum common SINR, i.e., $\text{SINR}^{(c)} = \min_k\{\text{SINR}_k^{(c)}\}$. Assuming that common message can be decoded without error, the achievable private SINR is

$$\text{SINR}_k^{(p)} = \frac{tP|h_{k,k}|^2}{\sigma_n^2}. \tag{10}$$

So the average common and private rate can be represented as the functions with respect to power allocation factor, t,

$$R^{(c)} = \mathbb{E}\left\{\log_2\left(1 + \text{SINR}^{(c)}\right)\right\}, \tag{11}$$

$$R_k^{(p)} = \mathbb{E}\left\{\log_2\left(1 + \text{SINR}_k^{(p)}\right)\right\}. \tag{12}$$

Obviously, the perfect global CSIT is necessary for the perfect alignment between the private and common desired signals, and the complete cancellation of ICI at RXs. Due to the limited fronthaul and feedback links, perfect acquisition of CSIT is not a straightforward task in practice. In the following subsections, the imperfect CSIT model is detailed.

B. CSIT QUANTIZATION ERROR MODEL

To reduce the amount of information exchanged for CSI sharing under such limited fronthaul and feedback links, the codebook-based quantization technique is required. Specifically, for the channel $\mathbf{H}_{k,j}$, it is first vectorized as $\mathbf{h}_{k,j} = \text{vec}(\mathbf{H}_{k,j})$, then TX j selects an optimal code word from a predetermined codebook $\mathcal{H}_j = [\hat{\mathbf{h}}_j^{(1)}, \ldots, \hat{\mathbf{h}}_j^{(2^B)}]$ of size 2^B based on the following criterion

$$c_0 = \arg\max_{1\leq i\leq 2^B}\left|\tilde{\mathbf{h}}_{k,j}^{\text{H}}\hat{\mathbf{h}}_j^{(i)}\right|^2, \tag{13}$$

where i.i.d. code word $\hat{\mathbf{h}}_j^{(i)} \sim \mathcal{CN}(0, \mathbf{I}_{N_rN_t})$, B is the number of quantization bits and $\tilde{\mathbf{h}}_{k,j} = \mathbf{h}_{k,j}/\|\mathbf{h}_{k,j}\|$ is channel direction vector. The quantization error is $\delta_{k,j} = 1 - |\tilde{\mathbf{h}}_{k,j}^{\text{H}}\hat{\mathbf{h}}_{k,j}|^2$, where $\hat{\mathbf{h}}_{k,j} = \hat{\mathbf{h}}_j^{(c_0)}$ is the quantized vector of $\mathbf{h}_{k,j}$. Following the theory of random vector quantization (RVQ), the expected value of $\delta_{k,j}$ is given by [19]

$$\xi = \mathbb{E}[\delta_{k,j}] = 2^B\beta\left(2^B, \frac{N_t}{Q}\right) \tag{14}$$

where $Q = N_tN_r - 1$ and $\beta(\cdot,\cdot)$ is Euler's Beta function. The relation between the actual direction vector $\tilde{\mathbf{h}}_{k,j}$ and the quantized one $\hat{\mathbf{h}}_{k,j}$ is

$$\tilde{\mathbf{h}}_{k,j} = \sqrt{1-\delta_{k,j}}\hat{\mathbf{h}}_{k,j} + \sqrt{\delta_{k,j}}\mathbf{e}_{k,j}, \tag{15}$$

where $\mathbf{e}_{k,j}$ is an unit-norm vector isotropically distributed in the null-space of $\hat{\mathbf{h}}_{k,j}$ and is independent of $\delta_{k,j}$. The vectorized channels are recovered to matrices, and then we have

$$\mathbf{H}_{k,j} = \|\mathbf{H}_{k,j}\|_{\text{F}}\left(\sqrt{1-\delta_{k,j}}\hat{\mathbf{H}}_{k,j} + \sqrt{\delta_{k,j}}\mathbf{E}_{k,j}\right), \tag{16}$$

where the equation is derived from $\|\mathbf{A}\|_F^2 = \|\text{vec}(\mathbf{A})\|^2$, $\hat{\mathbf{H}}_{k,j} = \text{rvec}(\hat{\mathbf{h}}_{k,j})$, and $\mathbf{E}_{k,j} = \text{rvec}(\mathbf{e}_{k,j})$, Thereafter, any variable dependent on the quantized channel vectors is denoted as a symbol with a hat above, i.e., $\hat{a}$.

III. PERFORMANCE ANALYSIS OF SIA-RS TRANSMISSION STRATEGY

Considering the quantization error, the average sum rate, outage probability and SER are derived in this section.

A. STATISTICAL CHARACTERISTICS OF KEY RANDOM VARIABLES

1) RESIDUAL INTERFERENCE POWER

The residual interference power due to CSI quantization error at RX k is

$$
\begin{aligned}
I_k^{(p)} &= tP \sum_{j\in\mathcal{K}\setminus\{k\}} \left|\hat{u}_k^{\mathrm{H}}\mathbf{H}_{k,j}\hat{\mathbf{v}}_j^{(p)}\right|^2 \\
&= tP \sum_{j\in\mathcal{K}\setminus\{k\}} \|\mathbf{h}_{k,j}\|^2 \left|\boldsymbol{\alpha}_{k,j}\tilde{\mathbf{h}}_{k,j}\right|^2 && \text{(17a)}\\
&= tP \sum_{j\in\mathcal{K}\setminus\{k\}} \|\mathbf{h}_{k,j}\|^2 \Big|\sqrt{1-\delta_{k,j}}\boldsymbol{\alpha}_{k,j}\hat{\mathbf{h}}_{k,j} \\
&\quad + \sqrt{\delta_{k,j}}\boldsymbol{\alpha}_{k,j}\mathbf{e}_{k,j}\Big|^2 && \text{(17b)}\\
&= tP \sum_{j\in\mathcal{K}\setminus\{k\}} \delta_{k,j}\|\mathbf{h}_{k,j}\|^2|\boldsymbol{\alpha}_{k,j}\mathbf{e}_{k,j}|^2 && \text{(17c)}\\
&\triangleq tP \sum_{j\in\mathcal{K}\setminus\{k\}} Q_{k,j}^{(p)}, && \text{(17d)}
\end{aligned}
$$

where $\boldsymbol{\alpha}_{k,j} = \hat{\mathbf{v}}_j^{(p)} \otimes \hat{\mathbf{u}}_k^{\mathrm{H}}$ with $\|\boldsymbol{\alpha}_{k,j}\|^2 = 1$ for $k, j \in \mathcal{K}$ []; (17b) is obtained by substituting (15) in to (17a); (17c) is based on IA condition in (3).

$\delta_{k,j}\|\mathbf{h}_{k,j}\|^2 \sim \mathrm{Gamma}(Q, 2^{-B/Q})$, $\forall k, j \in \mathcal{K}$ [20]. Since $\boldsymbol{\alpha}_{k,j}$ and $\mathbf{e}_{k,j}$ are independent, for $j \in \mathcal{K}$, $|\boldsymbol{\alpha}_{k,j}\mathbf{e}_{k,j}|^2$'s are independent and follow Beta$(1, Q-1)$. Therefore, $Q_{k,j}^{(p)} \sim 2^{-B/Q}\chi^2(2)$ [21], and thus $I_k^{(p)}$ is the weighted sum of exponential distribution random variables (RVs), following Erlang$(K-1, 2^{-B/Q})$.

2) PRIVATE DESIRED SIGNAL POWER

The private desired signal power at RX k is

$$
S_k^{(p)} = tP \left|\hat{\mathbf{u}}_k^{\mathrm{H}}\mathbf{H}_{k,k}\hat{\mathbf{H}}_{k,k}\hat{\mathbf{v}}_k^{(p)}\right|^2 = tP|\boldsymbol{\alpha}_{k,k}\mathbf{h}_{k,k}|^2. \quad (18)
$$

In the case of conventional IA, $\hat{\mathbf{u}}_k$ and $\hat{\mathbf{v}}_k^{(p)}$ are independent of direct link $\mathbf{H}_{k,k}$ along with its quantized version $\hat{\mathbf{H}}_{k,k}$, and only depend on interference channels $\{\hat{\mathbf{H}}_{k,j}, j \neq k, \forall j \in \mathcal{K}\}$. Thus, $|\boldsymbol{\alpha}_{k,k}\mathbf{h}_{k,k}|^2 \sim \chi^2(2)$ [22].

In the case of the proposed SIA-RS, the design of $\hat{\mathbf{u}}_k$ and $\hat{\mathbf{v}}_k^{(p)}$ depend on all the links to RX k, $\{\hat{\mathbf{H}}_{k,j}, j \in \mathcal{K}\}$ including direct link $\mathbf{H}_{k,k}$. In order to derive the distribution of private desired signal, the following theorem is introduced.

Proposition 1: If the common and private desired signals are aligned as (5), $\hat{\mathbf{u}}_k$ and $\hat{\mathbf{v}}_k^{(p)}$ depend on direct link $\mathbf{H}_{k,k}$. Let $|\hat{h}_{k,k}|^2 \triangleq \left|\hat{\mathbf{u}}_k^{\mathrm{H}}\hat{\mathbf{H}}_{k,k}\hat{\mathbf{v}}_k^{(p)}\right|^2$ and $\hat{\mathbf{g}}_k = \hat{\mathbf{H}}_{k,k}\hat{\mathbf{v}}_k^{(p)}$, then

$$
|\hat{h}_{k,k}|^2 \sim \chi^2(2), \quad \hat{\mathbf{g}}_k \sim \mathcal{CN}(\mathbf{0}, \mathbf{I}_{N_t}). \quad (19)
$$

Proof: The proof is detailed in Appendix A. □

According to Proposition 1, the private desired signal power at RX k is derived as follows,

$$
\begin{aligned}
S_k^{(p)} &= tP|\boldsymbol{\alpha}_{k,k}\mathbf{h}_{k,k}|^2 \\
&\approx tP\left\|\mathbf{h}_{k,k}\right\|^2 \left[(1-\delta_{k,k})\left|\boldsymbol{\alpha}_{k,k}\hat{\mathbf{h}}_{k,k}\right|^2 + \delta_{k,k}|\boldsymbol{\alpha}_{k,k}\mathbf{e}_{k,k}|^2\right] && \text{(20a)}\\
&\approx tP\Big[\mathbb{E}\{\underbrace{\|\mathbf{h}_{k,k}\|^2}_{\sim\chi^2(N_rN_t)} - \underbrace{\delta_{k,k}\|\mathbf{h}_{k,k}\|^2}_{\sim\mathrm{Gamma}(Q,2^{-B/Q})}\}|\hat{h}_{k,k}|^2 \\
&\quad + \underbrace{\delta_{k,k}\|\mathbf{h}_{k,k}\|^2|\boldsymbol{\alpha}_{k,k}\mathbf{e}_{k,k}|^2}_{\sim 2^{-B/Q}\chi^2(2)}\Big] && \text{(20b)}\\
&= tP(N_tN_r - Q2^{-B/Q})|\hat{h}_{k,k}|^2 + tPQ_{k,k}^{(p)} && \text{(20c)}
\end{aligned}
$$

where in (20a) the cross terms are omitted compared with other terms [21]; in (20b), since the product distribution of two correlated Gamma distributed RVs, $\|\mathbf{h}_{k,k}\|$ and $|\hat{h}_{k,k}|$, is difficult to obtain, $\|\mathbf{h}_{k,k}\|^2$ and $\delta_{k,k}\|\mathbf{h}_{k,k}\|^2$ are averaged to get $\mathbb{E}\{\|\mathbf{h}_{k,k}\|^2\} = N_rN_t$ and $\mathbb{E}\{\delta_{k,k}\|\mathbf{h}_{k,k}\|^2\} = Q2^{-B/Q}$, respectively. Equation (20c) implies that $S_k^{(p)}$ is a finite weighted sum of Erlang RVs.

3) COMMON SIGNAL POWER

Before the derivation of common signal power, the following lemma is introduced.

Lemma 1: For the coefficient $c_k^{(p)}$ in (6), with respect to $\hat{\mathbf{H}}_k$, we have approximation $\mathbb{E}\{c_k^{(p)2}\} \approx 1/KN_t$.

Proof: The proof is detailed in Appendix B □

$$
\begin{aligned}
S_k^{(c)} &= (1-t)P\Big|\sum_{j\in\mathcal{K}}\hat{\mathbf{u}}_k^{\mathrm{H}}\mathbf{H}_{k,j}\mathbf{v}_j^{(c)}\Big|^2 = (1-t)P\Big|\sum_{j\in\mathcal{K}}\boldsymbol{\beta}_{k,j}\mathbf{h}_{k,j}\Big|^2 \\
&\approx (1-t)P\Big[\sum_{j\in\mathcal{K}}(1-\delta_{k,j})\|\mathbf{h}_{k,j}\|^2\left|\hat{\mathbf{u}}_k^{\mathrm{H}}\hat{\mathbf{H}}_{k,j}\mathbf{v}_j^{(c)}\right|^2 + \sum_{j\in\mathcal{K}}\delta_{k,j}\|\mathbf{h}_{k,j}\|^2\left|\boldsymbol{\beta}_{k,j}\mathbf{e}_{k,j}\right|^2\Big] && \text{(21a)}\\
&\approx (1-t)P\Big[(N_rN_t - Q2^{-B/Q})\left|\hat{\mathbf{u}}_k^{\mathrm{H}}\hat{\mathbf{H}}_k\mathbf{v}^{(c)}\right|^2 + \sum_{j\in\mathcal{K}}Q_{k,j}^{(c)}\Big] && \text{(21b)}\\
&= (1-t)P\Big[KN_t(N_rN_t - Q2^{-B/Q})\left|\hat{\mathbf{u}}_k^{\mathrm{H}}\hat{\mathbf{H}}_{k,k}\mathbf{v}_k^{(p)}\right|^2 + \sum_{j\in\mathcal{K}}Q_{k,j}^{(c)}\Big] && \text{(21c)}\\
&= (1-t)P\Big[KN_t(N_rN_t - Q2^{-B/Q})\left|\hat{h}_{k,k}\right|^2 + \sum_{j\in\mathcal{K}}Q_{k,j}^{(c)}\Big] && \text{(21d)}
\end{aligned}
$$

For the super common message, the received power at RX k is as shown in (21), as shown at the bottom of the previous page, where $\boldsymbol{\beta}_{k,j} = \hat{\mathbf{v}}_j^{(c)} \otimes \hat{\mathbf{u}}^{\mathrm{H}}, \forall k, j \in \mathcal{K}$, and $Q_{k,j}^{(c)} \triangleq \delta_{k,j}\|\mathbf{h}_{k,j}\|^2 \left|\boldsymbol{\beta}_{k,j}\mathbf{e}_{k,j}\right|^2 \sim 2^{-B/Q}\chi^2(2)$ is the common signal alignment error from the quantization. The approximation in (21a) is from the omitted cross terms between quantized channels and errors. For simplification, (21b) is obtained with $\mathbb{E}\{(1-\delta_{k,j})\|\mathbf{h}_{k,j}\|^2\} = (N_rN_t - Q2^{-B/Q})$. (21c) is derived from the common and private signal alignment in (6) and Lemma 1. With Proposition 1, it is obvious that $S_k^{(c)}$ is also a nested finite weighted sum of Erlang RVs.

For the convenience of notation, let $X \triangleq \eta_x|\hat{h}_{k,k}|^2 \sim \text{Erlang}(1, \eta_x)$ with $\eta_x \triangleq N_tN_r - Q2^{-B/Q}$, $Y_j \triangleq Q_{k,j}^{(p)} \sim \text{Erlang}(1, 2^{-B/Q})$, $Z_j \triangleq Q_{k,j}^{(c)} \sim \text{Erlang}(1, 2^{-B/Q})$, for $j \in \mathcal{K}$, and $Z \triangleq \sum_{j\in\mathcal{K}} Z_j \sim \text{Erlang}(K, 2^{-B/Q})$ with $\eta_z = K2^{-B/Q}$.

4) PDF OF NESTED FINITE WEIGHTED SUM OF ERLANG RANDOM VARIABLES

As mentioned before, the signal and interference power can be written as the nested finite weighted sum of Erlang RVs with the probability density function (PDF) obtained via the following lemma.

Lemma 2 [23]: Let $\{Y_l\}_{l=1}^L$ be a set of independent RVs following the PDF of Erlang distribution, where $Y_l \sim \text{Erlang}(m_l, \eta_l)$, $\forall l = \{1, \ldots, L\}$, and $\eta_i \neq \eta_j$, $\forall i \neq j$. Then the PDF of the sum $Z_L = \sum_{i=1}^L Y_i$ is a nested finite weighted sum of Erlang PDFs, given by

$$f_{Z_L}(z) = \sum_{i=1}^{L}\sum_{k=1}^{m_i} \Xi_L(i, k, \{m\}_{q=1}^L, \{\eta\}_{q=1}^{L-2}, \{l_q\}_{q=1}^{L-2}) \times f_{Y_i}(z; k, \eta_i), \tag{22}$$

where the weights Ξ_L are shown as follows

$$\begin{aligned}
&\Xi_L(i, k, \{m_i\}_{q=1}^L, \{\eta_i\}_{q=1}^L, \{l_i\}_{q=1}^{L-2}) \\
&= \sum_{l_1=k}^{m_i}\sum_{l_2=k}^{l_1}\cdots\sum_{l_{L-2}=k}^{l_{L-3}}\Bigg[\frac{(-1)^{R_L-m_i}\eta_i^k}{\prod_{h=1}^L \eta_h^{m_h}} \\
&\times \frac{(m_i + m_{1+\mathrm{U}(1-i)} - l_1 - 1)!}{(m_{1+\mathrm{U}(1-i)} - 1)!(m_i - l_1)!} \\
&\times \left(\frac{1}{\eta_i} - \frac{1}{\eta_{1+\mathrm{U}(1-i)}}\right)^{l_1 - m_i - m_{1+\mathrm{U}(1-i)}} \\
&\times \frac{(l_{L-2} + m_{L-1+\mathrm{U}(L-1-i)} - k - 1)!}{(m_{L-1+\mathrm{U}(L-1-i)} - 1)!(l_{L-2} - k)!} \\
&\times \left(\frac{1}{\eta_i} - \frac{1}{\eta_{L-1+\mathrm{U}(L-1-i)}}\right)^{k - l_{L-2} - m_{L-1+\mathrm{U}(L-1-i)}} \\
&\times \prod_{s=1}^{L-3} \frac{(l_s + m_{s+1+\mathrm{U}(s+1-i)} - l_{s+1} - 1)!}{(m_{s+1+\mathrm{U}(s+1-i)} - 1)!(l_s - l_{s+1})!} \\
&\times \left(\frac{1}{\eta_i} - \frac{1}{\eta_{s+1+\mathrm{U}(s+1-i)}}\right)^{l_{s+1} - l_s - m_{s+1+\mathrm{U}(s+1-i)}}\Bigg],
\end{aligned} \tag{23}$$

$R_L \triangleq \sum_{i=1}^L m_i$ and PDF of Erlang distributed RV V_i is

$$f_{V_i}(z; k, \eta_i) = \frac{z^{k-1}}{\eta_i^k (k-1)!}\exp\left(-\frac{z}{\eta_i}\right)\mathrm{U}(z), \tag{24}$$

with $\mathrm{U}(x)$ is the unit step function defined as $\mathrm{U}(x \geq 0) = 1$ and zero otherwise.

The following lemma provides the expectation of RV $\ln(1 + Z_L)$ with Z_L as defined in Lemma 2.

Lemma 3 [23]: The RV Z_L is a nested finite weighted sum of Erlang PDFs defined in Lemma 2, $\int_0^\infty \ln(1+z) f_{Z_L}(z)dz$ is given by (25), as shown at the bottom of the page, where $\binom{k-1}{w-1} = \frac{(k-1)!}{(w-1)!(k-w)!}$, ${}_2F_2$ is a generalized hypergeometric series, and $\mathcal{C} \approx 0.5772$ is Euler's constant [24, (9.73)].

B. AVERAGE SUM RATE

If each RX target rate is allocated opportunistically based on the channel conditions, it makes sense to analyze the performance of sum rate. Under imperfect CSIT, the achievable average sum rate is

$$\bar{R}_{\text{sum}} = \mathbb{E}\left\{\sum_{k\in\mathcal{K}} R_k^{(p)} + \min_{k\in\mathcal{K}} R_k^{(c)}\right\} \triangleq \sum_{k\in\mathcal{K}} \bar{R}_k^{(p)} + \min_{k\in\mathcal{K}} \bar{R}_k^{(c)} \tag{26}$$

1) AVERAGE PRIVATE RATE

The residual interference from private signals is treated as additional Gaussian noise without considering its distribution [25]. Then, RX k's average private rate is

$$\begin{aligned}
\bar{R}_k^{(p)} &= \frac{1}{\ln 2}\mathbb{E}\left\{\ln\left(1 + \frac{S_k^{(p)}}{\sigma_n^2 + \mathbb{E}\{I_k^{(p)}\}}\right)\right\} \\
&= \frac{1}{\ln 2}\mathbb{E}\left\{\ln\left(1 + \frac{tPX + tPY_k}{\sigma_n^2 + (K-1)2^{-B/Q}tP}\right)\right\} \quad (27)\\
&\triangleq \frac{1}{\ln 2}\mathbb{E}\left\{\ln\left(1 + \frac{tPX + tPY_k}{\sigma_p^2}\right)\right\}, \quad (28)
\end{aligned}$$

$$\begin{aligned}
&\int_0^\infty \ln(1+z) f_{Z_L}(z)dz \\
&= \frac{1}{\ln 2}\sum_{i=1}^{L}\sum_{k=1}^{m_i} \Xi_L(i, k, \{m_i\}_{q=1}^L, \{\eta_i\}_{q=1}^L, \{l_i\}_{q=1}^{L-2}) \frac{1}{(k-1)!}\left(\frac{1}{\eta_i}\right)^k \sum_{w=1}^{k}\binom{k-1}{w-1}(-1)^{k-w}\exp\left(\frac{1}{\eta_i}\right) \\
&\times \left\{\frac{1}{w^2}{}_2F_2\left(w, w; w+1, w+1; -\frac{1}{\eta_i}\right) + \eta_i^w (w-1)!\left[\ln(\eta_i) + \sum_{h=1}^{w-1}\frac{1}{h} - \mathcal{C}\right]\right\}
\end{aligned} \tag{25}$$

where (27) is from the expectation of $I_k^{(p)} \sim \text{Erlang}(K-1, 2^{-B/Q}tP)$, and thus the equivalent noise power is $\sigma_p^2 = (K-1)2^{-B/Q}tP + \sigma_n^2$

Then, (28) is rewritten as $\triangleq \mathbb{E}\{\log_2(1+\zeta_k^{(p)})\}$ with SNR $\zeta_k^{(p)}$. Furthermore, we have

$$\zeta_k^{(p)} = \frac{tP}{\sigma_p^2}X + \frac{tP}{\sigma_p^2}Y \triangleq A_1 + A_2, \tag{29}$$

where $A_1 \triangleq tP/\sigma_p^2 X \sim \text{Erlang}(1, \bar{\eta}_1)$, $A_2 \triangleq tP/\sigma_p^2 Y \sim \text{Erlang}(1, \bar{\eta}_2)$, $\bar{\eta}_1 \triangleq tP\eta_x/\sigma_p^2$, and $\bar{\eta}_2 \triangleq tP2^{-B/Q}/\sigma_p^2$. A_1 and A_2 are correlated since they are both dependent on $\hat{\mathbf{h}}_{k,k}$. The following lemma gives the upper and lower bounds of the correlation coefficient ρ.

Lemma 4: The lower and upper bounds of the correlation coefficient between two correlated RVs following exponential distribution are $\rho_{\max} = 1$ and $\rho_{\min} = 1 - \pi^2/6$, respectively.

Proof: Probability integral transformation is used to construct counter-monotonic and co-monotonic exponential RVs, detailed in Appendix C. □

Because $\zeta_k^{(p)}$ is the nested finite weighted sum of correlated Erlang RVs, the following lemma is introduced to obtain $\zeta_k^{(p)}$'s distribution.

Lemma 5 [26]: Let $\mathbf{w}_l = [W_{l,1}, W_{l,2}]^{\mathrm{T}}$ with i.i.d. elements $W_{l,k} \sim \mathcal{N}(0, \bar{\eta}_l/2)$, $\forall l, k \in \infty, \in$. For $\mathbf{w} \triangleq [\mathbf{w}_1^{\mathrm{T}}, \mathbf{w}_2^{\mathrm{T}}]^{\mathrm{T}}$, the co-variance matrix is

$$\mathcal{K}_W = \mathbb{E}\{\mathbf{w}\mathbf{w}^{\mathrm{H}}\} = \begin{bmatrix} \eta_1/2 & 0 & \frac{\rho_{1,2}\sqrt{\bar{\eta}_1\bar{\eta}_2}}{2} & 0 \\ 0 & \eta_1/2 & 0 & \frac{\rho_{1,2}\sqrt{\bar{\eta}_1\bar{\eta}_2}}{2} \\ \frac{\rho_{2,1}\sqrt{\bar{\eta}_1\bar{\eta}_2}}{2} & 0 & \bar{\eta}_2/2 & 0 \\ 0 & \frac{\rho_{2,1}\sqrt{\bar{\eta}_1\bar{\eta}_2}}{2} & 0 & \bar{\eta}_2/2 \end{bmatrix}, \tag{30}$$

The relation between the co-variance of $A_1 \sim Erlang(1, \bar{\eta}_1)$, $A_2 \sim Erlang(1, \bar{\eta}_2)$ and the correlation of the elements of $\mathbf{w}$ is $\rho_{A_1,A_2} = \rho_{1,2}^2 \triangleq \rho$. Let $\{\lambda_1, \lambda_2\}$ are two distinct eigenvalues of $\mathcal{K}_W$, i.e.,

$$\lambda_1, \lambda_2 = \frac{1}{2}\left(\frac{\bar{\eta}_1}{2}+\frac{\bar{\eta}_2}{2}\right) \pm \frac{1}{2}\sqrt{\left(\frac{\bar{\eta}_1}{2}+\frac{\bar{\eta}_2}{2}\right)^2 - \bar{\eta}_1\bar{\eta}_2(1-\rho^2)}. \tag{31}$$

Based on above assumption, the sum of correlated Erlang distributed RVs can be rewritten as the sum of independent RVs, i.e.,

$$A_1 + A_2 \overset{d}{=} V_1 + V_2,$$

where $\overset{d}{=}$ means equality in distribution, and $V_l \sim Erlang(1, 2\lambda_l)$.

Based on Lemma 5, $\zeta_k^{(p)} = A_1 + A_2 \overset{d}{=} V_1 + V_2$, $V_1 \sim \text{Erlang}(1, 2\lambda_1)$, $V_2 \sim \text{Erlang}(1, 2\lambda_2)$, $\eta_1 \triangleq 2\lambda_1$, $\eta_2 \triangleq 2\lambda_2$, and $m_1 = m_2 = 1$. Therefore, RX k's average private rate can be derived from Lemma 3 as [23]

$$\begin{aligned}\bar{R}_k^{(p)} &= \frac{1}{\ln 2}\mathbb{E}\{\ln(1+\zeta_k^{(p)})\} \\ &= \frac{1}{\ln 2}\int_0^\infty \ln(1+z) f_{Z_2}(z)dz \\ &= -\frac{1}{\ln 2}\sum_{i=1}^{2}\frac{1}{\eta_{1+\mathrm{U}(1-i)}}\left(\frac{1}{\eta_i} - \frac{1}{\eta_{1+\mathrm{U}(1-i)}}\right)^{-1} \\ &\quad \times \exp\left(\frac{1}{\eta_i}\right)\mathrm{Ei}\left(-\frac{1}{\eta_i}\right),\end{aligned} \tag{32}$$

where

$$f_{Z_2}(z) = \sum_{i=1}^{2}\sum_{k=1}^{m_i}\Xi_2(i,k,m_1,m_2,\eta_1,\eta_2) f_{V_i}(z;k,\eta_i),$$

$\Xi_2(i,k,m_1,m_2,\eta_1,\eta_2)$ is given in (33), as shown at the bottom of the page, $\mathrm{Ei}(x) = -\int_{-x}^{\infty} t^{-1}e^{-t}dt$ is the exponential integral function, satisfying the relationship with ${}_2F_2$

$$\Xi_2(i,k,m_1,m_2,\eta_1,\eta_2) = \frac{(-1)^{m_1+m_2-m_i}\eta_i^k(m_1+m_2-k-1)!}{\eta_1^{m_1}\eta_2^{m_2}(m_{1+\mathrm{U}(1-i)}-1)!(m_i-k)!}\left(\frac{1}{\eta_i} - \frac{1}{\eta_{1+\mathrm{U}(1-i)}}\right)^{k-m_1-m_2} \tag{33}$$

$$\begin{aligned}\mathbb{E}\left\{\ln(1+\zeta_k^{(c)})\right\} &\approx \int_0^\infty \ln(1+z) f_{Z_3}(z)dz \\ &= \sum_{i=1}^{3}\sum_{k=1}^{m_i}\Xi_3(i,k,m_1,m_2,m_3,\eta_1,\eta_2,\eta_3)\frac{1}{(k-1)!}\left(\frac{1}{\eta_i}\right)^k\sum_{w=1}^{k}\binom{k-1}{w-1}(-1)^{k-w}\exp\left(\frac{1}{\eta_i}\right) \\ &\quad \times \left\{\frac{1}{w^2}{}_2F_2\left(w,w;w+1,w+1;-\frac{1}{\eta_i}\right) + \eta_i^w(w-1)!\left[\ln(\eta_i) + \sum_{h=1}^{w-1}\frac{1}{h} - \mathcal{C}\right]\right\}\end{aligned} \tag{34}$$

$$\begin{aligned}\Xi_3(i,k,m_1,m_2,m_3,\eta_1,\eta_2,\eta_3,l_1) = \sum_{l_1=k}^{m_i}(-1)^{K+2-m_i}\frac{\eta_i^k(m_i+m_{1+\mathrm{U}(1-i)}-l_1-1)!}{\eta_1^{m_1}\eta_2^{m_2}\eta_3^{m_3}(m_{1+\mathrm{U}(1-i)}-1)!(m_i-l_1)!}\left(\frac{1}{\eta_i} - \frac{1}{\eta_{1+\mathrm{U}(1-i)}}\right)^{l_1-m_i-m_{1+\mathrm{U}(1-i)}} \\ \times \frac{(l_1+m_{2+\mathrm{U}(2-i)}-k-1)!}{(m_{2+\mathrm{U}(2-i)}-1)!(l_1-k)!}\left(\frac{1}{\eta_i} - \frac{1}{\eta_{2+\mathrm{U}(2-i)}}\right)^{k-l_1-m_{2+\mathrm{U}(2-i)}}\end{aligned} \tag{35}$$

[24, (9.14.1)] as follows,

$${}_2F_2(1, 1; 2, 2; -1/\eta_i) = \eta_i(\mathcal{C} + \ln(1/\eta_i) - \mathrm{Ei}(-1/\eta_i)).$$

2) AVERAGE COMMON RATE

Consider the statistical characteristics of $R^{(c)} = \min_{k\in\mathcal{K}}\{R_k^{(c)}\}$. Let $M_K \triangleq R^{(c)}$ and $C_k \triangleq R_k^{(c)}$, $\forall k \in \mathcal{K}$. $\{C_k\}_{k\in\mathcal{K}}$ follow the identical distribution.

In the light of [27], M_K's the cumulative distribution function (CDF) can be approximated by its upper bound,

$$F_{M_K}(x) \le 1 - (1 - F_C(x))^K, \tag{36}$$

which results from $\Pr(M_K \ge x) = \Pr(C_1 \ge x, \ldots, C_K \ge x) \le \Pr(C_1 \ge x)\ldots\Pr(C_K \ge x)$. The expected value of M_K is approximated by

$$\begin{aligned}\bar{R}^{(c)} &= \mathbb{E}\{M_K\} \approx \int_0^\infty (1 - F_C(x))^K dx\\ &= \sum_{n=1}^{K}\binom{K}{n}(-1)^n\int_0^\infty (F_C(x))^n dx,\end{aligned} \tag{37}$$

which is due to power expansion of $(1-x)^K$ for $x \in [0, 1]$.

Derived from Lemma 2, the CDF of the nested weighted sum of Erlang RVs, F_C, is given by

$$F_C(x) = \sum_{i=1}^{L}\sum_{k=1}^{m_i}\Xi_L(i, k, \{m_i\}_{q=1}^{L}, \{\eta_i\}_{q=1}^{L}, \{l_i\}_{q=1}^{L-2}) \times F_{A_i}(x; k, \eta_i), \tag{38}$$

where $A_i \sim \mathrm{Erlang}(m_i, \eta_i)$, $i \in \{1, 2, \ldots, L\}$,

$$F_{A_i}(x; m_i, \eta_i) = \left[1 - \exp\left(\frac{x}{\eta_i}\right)\sum_{\mu=1}^{m_i-1}\frac{1}{\mu!}\left(\frac{x}{\eta_i}\right)^{\mu}\right]\mathrm{U}(x).$$

Obviously, the integral in (37) is very difficult to solve after substituting (38) into (37).

With Jensen inequality, $\mathbb{E}\{\min_k\{R_k^{(c)}\}\} \ge \min_k\{\mathbb{E}\{R_k^{(c)}\}\}$, where function $f(x) = \min_i(x_i)$ is convex. Hence, let $\bar{R}^{(c)} \approx \min_k\{\bar{R}_k^{(c)}\}$ for simplification.

Similar to the private rate, treating the residual interference as noise, RX k's average common rate is given by

$$\begin{aligned}\bar{R}_k^{(c)} &= \frac{1}{\ln 2}\mathbb{E}\left\{\ln\left(1 + \frac{S_k^{(c)}}{\sigma_p^2} + \frac{S_k^{(p)}}{\sigma_p^2}\right) - \ln\left(1 + \frac{S_k^{(p)}}{\sigma_p^2}\right)\right\}\\ &= \frac{1}{\ln 2}\mathbb{E}\Bigg\{\ln\bigg(\frac{P}{\sigma_p^2}((1-t)KN_t + t)X\\ &\quad + \frac{(1-t)P}{\sigma_p^2}\sum_{j\in\mathcal{K}}Z_j + \frac{tP}{\sigma_p^2}Y_k + 1\bigg)\Bigg\} - \bar{R}_k^{(p)}\\ &\triangleq \frac{1}{\ln 2}\mathbb{E}\left\{\ln(1 + \zeta_k^{(c)})\right\} - \bar{R}_k^{(p)},\end{aligned} \tag{39}$$

where $\zeta_k^{(c)} \triangleq A_1 + A_2 + A_3$, $A_1 \sim \mathrm{Erlang}(1, ((1-t)KN_t) + t)\eta_x P/\sigma_p^2)$, $A_2 \sim \mathrm{Erlang}(K, (1-t)P2^{-B/Q}/\sigma_p^2)$, and $A_3 \sim \mathrm{Erlang}(1, tP2^{-B/Q}/\sigma_p^2)$. A_1, A_2 and A_3 are correlated due to the dependence on $\{\hat{\mathbf{H}}_{k,j}\}$. And thus the first term in (39) is the nested finite weighted sum of correlated Erlang RVs. Theorem 2 in [23] can be employed to handle any number of correlated RVs. Reference [8] proves that correlated common and private power can be approximated by the distribution of uncorrelated random variables. Therefore, the nested finite weighted sum of independent Erlang RVs are used for approximation, which means that (39)'s first term is given by (34), as shown at the bottom of the previous page, where $m_1 = 1$, $m_2 = K$, $m_3 = 1$, $\eta_1 = ((1-t)KN_t + t)P\eta_x/\sigma_p^2$, $\eta_2 = (1-t)P2^{-B/Q}/\sigma_p^2$, $\eta_3 = tP2^{-B/Q}/\sigma_p^2$,

$$f_{Z_3}(z) = \sum_{i=1}^{3}\sum_{k=1}^{m_i}\Xi_3(i, k, m_1, m_2, m_3, \eta_1, \eta_2, \eta_3, l_1) \times f_{A_i}(z; k, \eta_i),$$

and $\Xi_3(i, k, m_1, m_2, m_3, \eta_1, \eta_2, \eta_3, l_1)$ is given by (35), as shown at the bottom of the previous page.

In consequence, the average sum rate is achieved by substituting the average private rate in (32) and common one in (39) into (26).

C. OUTAGE PROBABILITY

In a latency-sensitive network, each transmitter transmits the messages at a fixed rate. Let the target rates to be $\{R_k^* = R_k^{(c)*} + R_k^{(p)*}\}_{k\in\mathcal{K}}$, including the common target rate $\{R_k^{(c)*}\}_{k\in\mathcal{K}}$ and private target rate $\{R_k^{(p)*}\}_{k\in\mathcal{K}}$. If the common message is not decoded successfully, then it is likely that the private messages cannot be decoded. it is assumed that if any one of the following two conditions is satisfied, RX k will encounter the outage event:

- RX k fails to decode the common message, i.e., $R_k^{(c)} \le \sum_{j\in\mathcal{K}} R_j^{(c)*}$;
- RX k decodes the common message while fails to detect the private message, i.e., $R_k^{(c)} \ge \sum_{j\in\mathcal{K}} R_j^{(c)*}$, and $R_k^{(p)} \le R_k^{(p)*}$.

So RX k's outage probability is

$$P_k^o = \Pr\left\{\left(R_k^{(c)} \ge \sum_{j\in\mathcal{K}} R_j^{(c)*}\right) \cap \left(R_k^{(p)} \le R_k^{(p)*}\right)\right\} + \Pr\left\{R_k^{(c)} \le \sum_{j\in\mathcal{K}} R_j^{(c)*}\right\}. \tag{40}$$

If RX k is unable to decode common message, then

$$\begin{aligned}\mathrm{SINR}_k^{(c)} &\triangleq \frac{S_k^{(c)}}{S_k^{(p)} + \sigma_p^2}\\ &= \frac{(1-t)\left(KN_t\eta_x|\hat{h}_{k,k}|^2 + \sum_{j\in\mathcal{K}} Q_{k,j}^{(c)}\right)}{t\left(\eta_x|\hat{h}_{k,k}|^2 + Q_{k,k}^{(p)}\right) + \sigma_p^2/P} \le \gamma^{(c)}\end{aligned} \tag{41}$$

$$\Rightarrow \eta_x|\hat{h}_{k,k}|^2 \le \frac{\gamma^{(c)}tQ_{k,k}^{(p)} - (1-t)\sum_{j\in\mathcal{K}} Q_{k,j}^{(c)} + \frac{\gamma^{(c)}\sigma_p^2}{P}}{(1-t)KN_t - \gamma^{(c)}t} \tag{42}$$

$$\Rightarrow X \leq a_1(t)Y_k - a_2(t)\sum_{j\in\mathcal{K}} Z_j + a_0(t) \triangleq a(y, \mathbf{z}), \tag{43}$$

where $\gamma^{(c)} \triangleq 2^{\sum_{j\in\mathcal{K}} R_j^{(c)*}} - 1$. Analogously, if RX k is unable to decode the private message, the following inequalities need to be satisfied.

$$\mathrm{SINR}_k^{(p)} \triangleq \frac{S_k^{(p)}}{\sigma_p^2} = \frac{\eta_x|\hat{h}_{k,k}|^2 + Q_{k,k}^{(p)}}{\sigma_p^2/(tP)} \leq \gamma_k^{(p)} \tag{44}$$

$$\Rightarrow \eta_x|\hat{h}_{k,k}|^2 \leq \gamma_k^{(p)}\frac{\sigma_p^2}{tP} - Q_{k,k}^{(p)} \tag{45}$$

$$\Rightarrow X \leq -Y_k + b_0(t) \triangleq b(y) \tag{46}$$

where $\gamma_k^{(p)} \triangleq 2^{R_k^{(p)*}} - 1$. To guarantee that decoding failure of the common message will result in that of the private one, we have $a(y, \mathbf{z}) \leq b(y)$, where the relationship is valid with some probability given by the following proposition.

Proposition 2: The probability of the event that decoding failure of the common message will result in that of the private one is given by

$$\Pr\{a(y, \mathbf{z}) \leq b(y)\} \approx 1 - \exp\left(\left[\frac{\gamma^{(c)}(\gamma_k^{(p)}+1)}{(1-t)KN_t} - \frac{\gamma_k^{(p)}}{t}\right]\frac{\sigma_p^2}{P}2^{B/Q}\right). \tag{47}$$

In the high-SNR regime, $\Pr\{a(y, \mathbf{z})\} \leq b(y) \rightarrow 1$. *In the low-SNR regime, if the power allocation between common and private parts satisfies the following inequality*

$$\frac{1-t}{t} \geq \frac{\gamma^{(c)}(\gamma_k^{(p)}+1)}{KN_t\gamma_k^{(p)}}, \tag{48}$$

then $\Pr\{a(y, \mathbf{z}) \leq b(y)\} \rightarrow 1$.

Proof:

$$\begin{aligned}&\Pr\{a(y, \mathbf{z}) \leq b(y)\}\\ &= \Pr\left\{Y_k \leq \frac{a_2}{a_1+1}\sum_{j\in\mathcal{K}} Z_j + \frac{b_0 - a_0}{a_1+1}\right\}\\ &\triangleq \Pr\{Y_k \leq Z + C\} = \int_0^\infty F_Y(z+C)f_Z(z)dz,\end{aligned} \tag{49}$$

where $Y_k \sim \mathrm{Erlang}(1, \eta_y)$ with $\eta_y \triangleq 2^{-B/Q}$ and $Z \sim \mathrm{Erlang}(K, \eta_z)$ with $\eta_z \triangleq 2^{-B/Q}a_2/(a_1+1)$. CDF and PDF of Y and Z are,

$$F_Y(y) = 1 - \exp\left(-\frac{y}{\eta_y}\right) \tag{50}$$

$$f_Z(z) = \frac{1}{\eta_z^K(K-1)!}z^{K-1}\exp\left(-\frac{z}{\eta_z}\right) \tag{51}$$

Substituting (50) and (51) into (49), we have

$$\begin{aligned}&\int_0^\infty F_Y(z+C)f_Z(z)dz\\ &= 1 - \frac{\int_0^\infty z^{K-1}\exp\left(-\left(\frac{1}{\eta_y}+\frac{1}{\eta_z}\right)z\right)dz}{\eta_z^K(K-1)!\exp\left(\frac{C}{\eta_y}\right)}\end{aligned}$$

$$= 1 - \frac{\Gamma(K)}{\eta_z^K(K-1)!\exp\left(\frac{C}{\eta_y}\right)\left(\frac{1}{\eta_y}+\frac{1}{\eta_x}\right)^K} \tag{52a}$$

$$= 1 - \frac{(KN_t)^K}{(KN_t+1)^K}\exp\left(\left[\frac{\gamma^{(c)}(\gamma_k^{(p)}+1)}{(1-t)KN_t} - \frac{\gamma_k^{(p)}}{t}\right]\times\frac{\sigma_p^2}{P}2^{B/Q}\right) \tag{52b}$$

$$\approx 1 - \exp\left(\left[\frac{\gamma^{(c)}(\gamma_k^{(p)}+1)}{(1-t)KN_t} - \frac{\gamma_k^{(p)}}{t}\right]\frac{\sigma_p^2}{P}2^{B/Q}\right), \tag{52c}$$

where (52a) is resulted from the formula [24, (3.381.4)]

$$\int_0^\infty x^{K-1}\exp(-ax)dx = a^{-K}\Gamma(K);$$

(52b) is derived from $\Gamma(K) = (K-1)!$; (52c) is approximated by $KN_t \gg 1$.

Let $\Upsilon \triangleq P/\sigma_p^2$ to be each RX's achievable SNR, satisfying $\Upsilon \geq \gamma_k \triangleq 2^{R_k^*-1}$. The asymptotic behaviour of (52c) with respect to (w.r.t.) Υ is as follows:

- For $\Upsilon \rightarrow \infty$, $\Pr(a \leq b) \rightarrow 1$, which means that in the high-SNR regime, if the common message cannot be decoded successfully, then private part won't either.
- For $\Upsilon \rightarrow 0$, to guarantee that the exponent in (52c) tends to 0, the coefficient of σ_p^2/P needs to be negative, that is,

$$\frac{\gamma^{(c)}(\gamma_k^{(p)}+1)}{(1-t)KN_t} \leq \frac{\gamma_k^{(p)}}{t} \Rightarrow \frac{1-t}{t} \geq \frac{\gamma^{(c)}(\gamma_k^{(p)}+1)}{KN_t\gamma_k^{(p)}}. \tag{53}$$

In the low-SNR regime, the power allocation between common and private parts is beneficial to ensure that the common message is decoded first and then the private one. Furthermore, decoding private message successfully implies that the whole message is decoded successfully. □

Assuming that the power allocation factor satisfies Proposition 2, that is, $a(y, \mathbf{z}) \leq b(y)$, the outage event happens if the private message cannot be to decoded. Therefore, the outage probability is expressed as

$$\begin{aligned}P_k^o &= \Pr\left\{R_k^{(p)} \leq R_k^{(p)*}\right\} = \Pr\{X \leq b(y)\}\\ &= \int_0^\infty F_X(-y+b_0)f_Y(y)dy\\ &= \int_0^\infty \left(1 - \exp\left(-\frac{-y+b_0}{\eta_x}\right)\right)\frac{1}{\eta_y}\exp\left(-\frac{y}{\eta_y}\right)dy\\ &= 1 - \left[\exp\left(\frac{b_0}{\eta_x}\right)\left(1 - \frac{\eta_y}{\eta_x}\right)\right]^{-1}\\ &= 1 - \left[\exp\left(\frac{\gamma_k^{(p)}\sigma_p^2}{tP(N_tN_r - Q2^{-B/Q})}\right)\right.\\ &\quad\left.\times\left(1 - \frac{2^{-B/Q}}{N_tN_r - Q2^{-B/Q}}\right)\right]^{-1}.\end{aligned} \tag{54}$$

D. SER

The reliability performance that is characterized by symbol error rate (SER) will be analyzed in this section. For the given SINR, γ, the average SER is expressed as

$$\bar{P}_{\text{ser}} = \int_0^\infty P_{\text{ser}}(\gamma) f(\gamma) d\gamma, \tag{55}$$

where, P_{ser} denotes SER. Herein consider Binary Phase Shift Keying (BPSK), Quadrature PSK (QPSK), M-ray PSK (MPSK) and M-ray Quadrature Amplitude Modulation (M-QAM), the SER expressions are as (56) [22], as shown at the bottom of the page, where G denotes an integral function w.r.t. $\exp(-\omega\gamma)$, and (κ, ω, M) denote the modulation-specific parameters.

For easy derivation, assume that X, Y_k and $\{Z\}_{j\in\mathcal{K}}$ are independent, and $\bar{Y} \triangleq \|\boldsymbol{\alpha}_{k,k}\mathbf{h}_{k,k}\|^2 \sim \chi^2(2)$. Let $(\kappa_c, \omega_c, M_c)$ to be the common message's modulation parameters defined $P_{\text{set}}^{(c)}$, and $(\kappa_p, \omega_p, M_p)$ defined $P_{\text{ser}}^{(p)}$ for the private part.

The RX k's average common SER is given by

$$\bar{P}_{\text{ser},k}^{(c)} = \iiint_0^\infty G\left(M, \kappa_c \exp\left(-\omega_c \frac{(1-t)KN_t x + (1-t)z}{ty + \sigma_p^2/P}\right)\right) \times f_X(x) f_{\bar{Y}}(y) f_Z(z) dx dy dz \tag{57}$$

First, integrate the exponential function in G w.r.t. z to get

$$\begin{aligned} &\frac{\kappa_c \exp\left(-\omega_c\left[\frac{(1-t)KN_t x}{ty+\sigma_p^2/P}\right]\right)}{\eta_z^K (K-1)!} \\ &\quad \times \int_0^\infty z^{K-1} \exp\left(-\left[\frac{(1-t)\omega_c}{ty+\sigma_p^2/P} + \frac{1}{\eta_z}\right]\right) dz \\ &= \frac{\kappa_c}{\eta_z^K} \exp\left(-\omega_c\left[\frac{(1-t)KN_t x}{ty+\sigma_p^2/P}\right]\right) \\ &\quad \times \left(\frac{(1-t)KN_t x}{ty+\sigma_p^2/P} + \frac{1}{\eta_z}\right)^{-K}, \end{aligned} \tag{58}$$

where (58) is derived from the formula [24, (3.381.4)].

Then, integrate (58) w.r.t. x to get

$$\begin{aligned} &\frac{\kappa_c}{\eta_z^K \eta_x} \left(\frac{(1-t)\omega_c}{ty+\sigma_p^2/P} + \frac{1}{\eta_z}\right)^{-K} \\ &\quad \times \int_0^\infty \exp\left(-\omega_c \frac{(1-t)KN_t}{ty+\sigma_p^2/P} x\right) \exp\left(-\frac{x}{\eta_x}\right) dx \\ &= \frac{\kappa_c}{\eta_z^K \eta_x} \left(\frac{(1-t)\omega_c}{ty+\sigma_p^2/P} + \frac{1}{\eta_z}\right)^{-K} \\ &\quad \times \left(\omega_c \frac{(1-t)KN_t}{ty+\sigma_p^2/P} + \frac{1}{\eta_x}\right)^{-1} \triangleq \phi(y). \end{aligned} \tag{59}$$

At last, integrate (59) w.r.t. y to get $\mathbb{E}\{\phi(y)\}$. However, the integral is too complicated to solve in a straightforward way. With Jensen inequality, for the convex function $\phi(y)$ (easy to prove), we have

$$\mathbb{E}\{\phi(y)\} \geq \phi(\mathbb{E}\{y\}) = \phi(1). \tag{60}$$

Therefore, the average common SER is expressed by

$$\begin{aligned} \bar{P}_{\text{ser},k}^{(c)} = G\Bigg(M_c, &\frac{\kappa_c}{\eta_z^K \eta_x} \left(\frac{(1-t)\omega_c}{t+\sigma_p^2/P} + \frac{1}{\eta_z}\right)^{-K} \\ &\times \left(\omega_c \frac{(1-t)KN_t}{t+\sigma_p^2/P} + \frac{1}{\eta_x}\right)^{-1}\Bigg), \end{aligned} \tag{61}$$

which is further solved via numerical integration. Similarly, the average private SER is given by

$$\bar{P}_{\text{ser},k}^{(p)} = G\left(M_p, \kappa_p \left(\frac{\omega_p t P}{\sigma_p^2} + 1\right)^{-1}\right). \tag{62}$$

IV. ASYMPTOTIC ANALYSIS OF PERFORMANCE LOSS

A. AVERAGE SUM RATE LOSS

Under perfect CSIT, the achievable average sum rate with conventional IA without RS is give by

$$\begin{aligned} \bar{R}_{\text{sum}}^{\text{perfect}} &= \sum_{j\in\mathcal{K}} \bar{R}_k^{\text{perfect}} \\ &= \sum_{j\in\mathcal{K}} \mathbb{E}\left\{\log_2\left(1 + \frac{P}{\sigma_n^2}\left|\mathbf{u}_k^{\text{H}}\mathbf{H}_{k,k}\mathbf{v}_k\right|^2\right)\right\}, \end{aligned} \tag{63}$$

where $\mathbf{u}_k$ and $\mathbf{v}_k$ are independent of $\mathbf{H}_{k,k}$, and thus $|\mathbf{u}_k^{\text{H}}\mathbf{H}_{k,k}\mathbf{v}_k|^2 \sim \chi^2(2)$,

$$\bar{R}_k^{\text{perfect}} = -\frac{1}{\ln 2} \exp\left(\frac{1}{\Upsilon}\right) \text{Ei}\left(-\frac{1}{\Upsilon}\right), \tag{64}$$

where $\Upsilon = P/\sigma_n^2$ denotes SNR.

Then, the average sum rate loss is defined as

$$\Delta R_{\text{sum}} = \bar{R}_{\text{sum}}^{\text{perfect}} - \bar{R}_{\text{sum}} = \sum_{j\in\mathcal{K}} \left(\bar{R}_k^{\text{perfect}} - \bar{R}_k^{(p)}\right) - \bar{R}^{(c)}. \tag{65}$$

$$P_{\text{ser}} = \begin{cases} \frac{1}{\pi}\int_0^{\frac{(M-1)\pi}{M}} \exp\left(-\frac{\sin^2(\pi/M)}{\sin^2(x)}\gamma\right) dx \triangleq G_{\text{PSK}}(M, \kappa\exp(-\omega\gamma)), & \text{M-PSK} \\ \frac{4}{\pi}\left(1 - \frac{1}{\sqrt{M}}\right)\left[\frac{1}{\sqrt{M}}\int_0^{\pi/4} \exp\left(-\frac{3}{2(M-1)\sin^2(x)}\gamma\right) dx \right. \\ \left. + \int_{\pi/2}^{\pi/4} \exp\left(-\frac{3}{2(M-1)\sin^2(x)}\gamma\right) dx\right] \triangleq G_{\text{QAM}}(M, \kappa\exp(-\omega\gamma)), & \text{M-QAM} \end{cases} \tag{56}$$

The asymptotic analysis of sum rate loss as SNR tends to positive infinity are shown as follows.

If SNR is sufficiently low, the system is noise-limited, and thus interference term can be omitted. Whether the CSIT is perfectly known or not has little effect on sum rate, and thus the sum rate loss can be ignored.

If SNR is sufficiently high, $\log(1+\Upsilon) \approx \log(\Upsilon)$. As for perfect CSIT, RX k's achievable asymptotic rate is

$$\bar{R}_k^{\text{perfect},(a)} \approx \frac{1}{\ln 2}\mathbb{E}\left\{\ln(\Upsilon|\mathbf{u}_k^{\mathrm{H}}\mathbf{H}_{k,k}\mathbf{v}_k|^2)\right\} = \frac{\ln(\Upsilon)-\mathcal{C}}{\ln 2}, \tag{66}$$

which use the formula $\int_0^\infty x^{k-1}\ln\exp(-\mu x)dx = 1/\eta^k\Gamma(k)[\Psi(k)-\ln\mu]$ [24, (4.331.1)], where $\Psi(k)$ is Euler Psi function defined by $\Psi(k) = d\ln\Gamma(k)/dx$ [24, (8.360.1)], $\Psi(1) = -\mathcal{C}$ [24, (8.360.5)].

In terms of the quantized CSIT, RX k's private asymptotic rate is given by (67), as shown at the bottom of the page, where (67b) is obtained by substituting $\eta_1 = tP\eta_x/\sigma_p^2$, $\eta_2 = tP2^{-B/Q}/\sigma_p^2$, $\eta_x = N_tN_r - Q2^{-B/Q}$ and $P/\sigma_p^2 \approx 1/((K-1)t2^{-B/Q})$ into (67a), which is independent of Υ.

In the similar way, the common asymptotic rate expression includes $\Psi(k)$ that varies with the number of RXs and difficult to compute. Therefore, average the common quantization error Z to eliminate the impact of its uncertainty on the result, and the common asymptotic rate is approximated by (68), as shown at the bottom of the page, where (68b) is obtained by substituting $\eta_z' = K(1-t)P/\sigma_p^2$, $\eta_1' = ((1-t)KN_t + t)P/(\sigma_p^2\eta_z')$ $\eta_2' = tP/(\sigma_p^2\eta_z')$ and $P/\sigma_p^2 \approx 1/((K-1)t2^{-B/Q})$ into (68a).

Therefore, the sum rate loss in high-SNR regime is given by (69), as shown at the bottom of the page, by substituting (66), (67b) and (68b) into (65).

There are following observations about (67b), (68b) and (69):

- In the high-SNR regime, the private asymptotic rate is related to B but not to t, which implies that private rate

$$\begin{aligned}
\bar{R}_k^{(p),(a)} &= \frac{1}{\ln 2}\sum_{i=1}^{2}\sum_{k=1}^{m_i}\Xi_2(i,k,m_1,m_2,\eta_1,\eta_2)\int_0^\infty \ln z\frac{z^{k-1}}{\eta_i(k-1)!}\exp\left(-\frac{z}{\eta_i}\right)dz \\
&= \frac{1}{\ln 2}\sum_{i=1}^{2}\sum_{k=1}^{1}\Xi_2(i,k,1,1,\eta_1,\eta_2)(\Psi(k)+\ln(\eta_i)) \\
&= -\frac{1}{\ln 2}\left[\frac{1}{\eta_2}\left(\frac{1}{\eta_1}-\frac{1}{\eta_2}\right)^{-1}(\ln\eta_1-\mathcal{C}) + \frac{1}{\eta_1}\left(\frac{1}{\eta_1}-\frac{1}{\eta_1}\right)^{-1}(\ln\eta_2-\mathcal{C})\right] \qquad (67a) \\
&= \frac{1}{\ln 2(N_tN_r-(Q+1)2^{-B/Q})}\left[(N_tN_r-Q2^{-B/Q})\left(\ln\left(\frac{N_tN_r-Q2^{-B/Q}}{(K-1)2^{-B/Q}}\right)-\mathcal{C}\right)-2^{-B/Q}\left(\ln\left(\frac{1}{K-1}\right)-\mathcal{C}\right)\right] \qquad (67b)
\end{aligned}$$

$$\begin{aligned}
&\bar{R}^{(c),(a)} + \bar{R}_k^{(p),(a)} \\
&\approx \frac{1}{\ln 2}\mathbb{E}\left\{\ln\left(\frac{P}{\sigma_p^2}((1-t)KN_t+t)X + \mathbb{E}\left\{\frac{(1-t)P}{\sigma_p^2}Z\right\} + \frac{tP}{\sigma_p^2}Y_k\right)\right\} \\
&= \frac{1}{\ln 2}\mathbb{E}\left\{\left(\frac{P}{\sigma_p^2\eta_z'}((1-t)KN_t+t)X + \frac{tP}{\sigma_p^2\eta_z'}Y_k + 1\right)\right\} + \frac{\ln(\eta_z')}{\ln 2} \\
&\approx \frac{1}{\ln 2}\sum_{i=1}^{2}\Xi_2(i,1,1,1,\eta_1',\eta_2')(\ln(\eta_i')-\mathcal{C}) + \frac{\ln\eta_z'}{\ln 2} \\
&= -\frac{1}{\ln 2}\left[\frac{1}{\eta_2'}\left(\frac{1}{\eta_1'}-\frac{1}{\eta_2'}\right)^{-1}(\ln(\eta_1')-\mathcal{C}) + \frac{1}{\eta_1'}\left(\frac{1}{\eta_2'}-\frac{1}{\eta_1'}\right)^{-1}(\ln(\eta_2')-\mathcal{C})\right] + \frac{\ln(\eta_z')}{\ln 2} \qquad (68a) \\
&= \frac{1}{\ln 2}\left[\left(1-\frac{t}{KN_t(1-t)}\right)\left(\ln\left(N_t+\frac{t}{K(1-t)}\right)-\mathcal{C}\right) - \frac{t}{KN_t(1-t)}\left(\ln\left(\frac{t}{K(1-t)}\right)-\mathcal{C}\right)\right. \\
&\quad \left. + \ln\left(\frac{K(1-t)}{(K-1)t2^{-B/Q}}\right)\right] \qquad (68b)
\end{aligned}$$

$$\begin{aligned}
f(t,B) \triangleq \Delta R_{\text{sum}}^{(a)} = \frac{1}{\ln 2}&\left\{K\ln(\Upsilon) - K\mathcal{C} - \frac{K-1}{N_tN_r-(Q+1)2^{-B/Q}}\left[(N_tN_r-Q2^{-B/Q})\left(\ln\left(\frac{(K-1)2^{-B/Q}}{N_tN_r-Q^{-B/Q}}\right)-\mathcal{C}\right)\right.\right. \\
&\left. - 2^{-B/Q}\left(\ln\left(\frac{1}{K-1}\right)-\mathcal{C}\right)\right] - \left[\left(1-\frac{t}{KN_t(1-t)}\right)\left(\ln\left(N_t+\frac{t}{K(1-t)}\right)-\mathcal{C}\right)\right. \\
&\left.\left. -\frac{t}{KN_t(1-t)}\left(\ln\left(\frac{t}{K(1-t)}\right)-\mathcal{C}\right)\right] - \ln\left(\frac{K(1-t)}{(K-1)t2^{-B/Q}}\right)\right\}. \qquad (69)
\end{aligned}$$

cannot be improved via adjusting the power allocation factor. For the given B, the CSIT quantization error will the bottleneck of the improvement of private rate as SNR increases.

- In the high-SNR regime, the common asymptotic rate is a function w.r.t. t and B, which implies that for the given B, while the private rate cannot be increased due to CSIT quantization error, the common rate will be increased via adjusting the power allocation factor, further achieving the enhanced performance of sum rate. This result illustrates that RS can reduce the sum rate loss from CSIT error and improve the robustness of transmission, especially for the high SNR.

B. OUTAGE PROBABILITY LOSS

Under the perfect CSIT, the outage probability is

$$P_k^{o,\text{perfect}} = \Pr\left\{R_k^{\text{perfect}} = R_k^*\right\} = 1 - \exp\left(-\frac{\gamma_k}{\Upsilon}\right). \tag{70}$$

The outage probability loss is given by

$$\begin{aligned}\Delta P_k^o &= P_k^o - P_k^{o,\text{perfect}} \\ &= \exp\left(-\frac{\gamma_k}{\Upsilon}\right) - \left[\exp\left(\frac{\gamma_k^{(p)}\sigma_p^2}{tP(N_tN_r - Q2^{-B/Q})}\right)\right. \\ &\quad \left.\times\left(1 - \frac{2^{-B/Q}}{N_tN_r - Q2^{-B/Q}}\right)\right]^{-1}.\end{aligned} \tag{71}$$

As $\Upsilon \to \infty$, $\sigma_p^2/P \to 0$. Therefore, asymptotic outage probability loss in the high-SNR regime is

$$\Delta P_k^{o,(a)} = 1 - \left[\left(1 - \frac{2^{-B/Q}}{N_tN_r - Q2^{-B/Q}}\right)\right]^{-1}. \tag{72}$$

There are the following observations about (71) and (72):

- In the low-SNR regime, the system is noise-limited, and thus the impact of residual interference term from imperfect CSIT on the outage probability can be omitted, that is, as $\Upsilon \to 0$, outage probability tends to 1.
- In the high-SNR regime, $\Delta P_k^{o,(a)}$ is a function of B, and independent of t, which means that for the given B, $\Delta P_k^{o,(a)}$ tends to a constant, and the power allocation between common and private parts for RS has no effect on lower the outage probability.
- For the given B, ΔP_k^o is a monotonically decreasing function of t. If $t = 1$, the outage probability loss is minimal, which implies that the conventional IA without RS can achieve better performance of outage probability. This is because the SIC process for RS increases the outage probability.

C. SER LOSS

Under the perfect CSIT, the average SER is given by

$$\bar{P}_{\text{ser},k}^{\text{perfect}} = G\left(M, \frac{\kappa}{\omega\Upsilon + 1}\right). \tag{73}$$

Because the common and private parts can employ the different modulation schemes and orders, it makes no sense that the SER of RS is compared with that of a unique modulation scheme and order under the perfect CSIT.

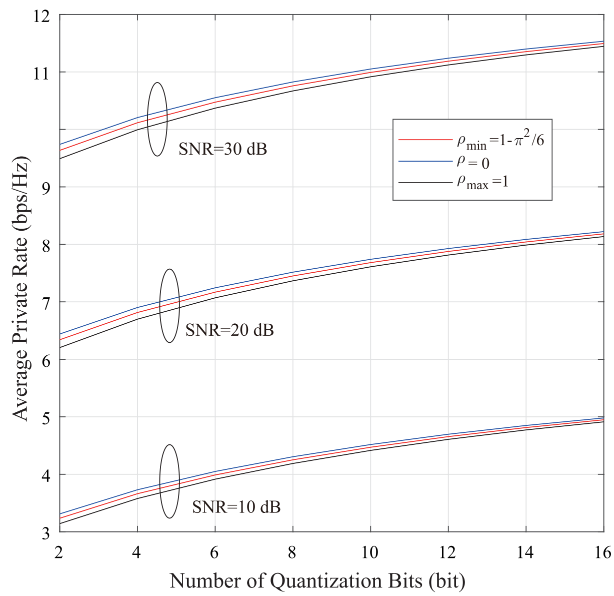

FIGURE 1. The impact of correlation coefficient ρ on average private rate versus B.

V. SIMULATION RESULTS AND DISCUSSIONS

This section presents the performance comparisons and analyses based on average sum rate, outage probability and SER closed-form expressions derived above. Consider $N_t = N_r = K = 3$, the private target SINR is $\gamma_k^{(p)} = \gamma^{(p)} = 1$, the total target SINR is $\gamma_k = \gamma = 2$, $\forall k \in \mathcal{K}$, and $\sigma_n^2 = 1$. The involved schemes include:

- *Conventional IA*, which doesn't perform signal alignment with $t = 1$,
- *Signal alignment based IA (SIA)* [18], which performs signal alignment with $t = 1$,
- *Conventional RS*, which doesn't perform signal alignment with $0 < t < 1$,
- *Proposed SIA-RS*, which performs signal alignment with $0 < t < 1$.

A. CORRELATION FROM SIGNAL ALIGNMENT

The average private rate derived in Section III-B1 involves two correlated RVs, desired and imperfectly aligned signals. The lower and upper bounds of the correlation coefficient are given by Lemma 5. We can observe from the simulation results in Fig. 1 that the derived average private rate has a relatively low sensibility on the correlation. Therefore, we can employ the independently Erlang distributed RVs to approximate the original ones.

B. AVERAGE SUM RATE

Fig. 2 compares the average sum rate among conventional IA, SIA, conventional RS and SIA-RS under the different SNR and the number of quantization bits B. First, average

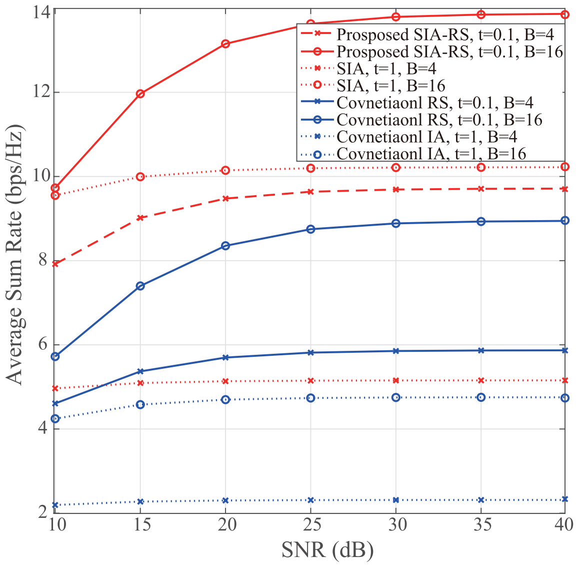

FIGURE 2. Comparison of average sum rate versus SNR among various schemes with $B = 4$ or $B = 16$.

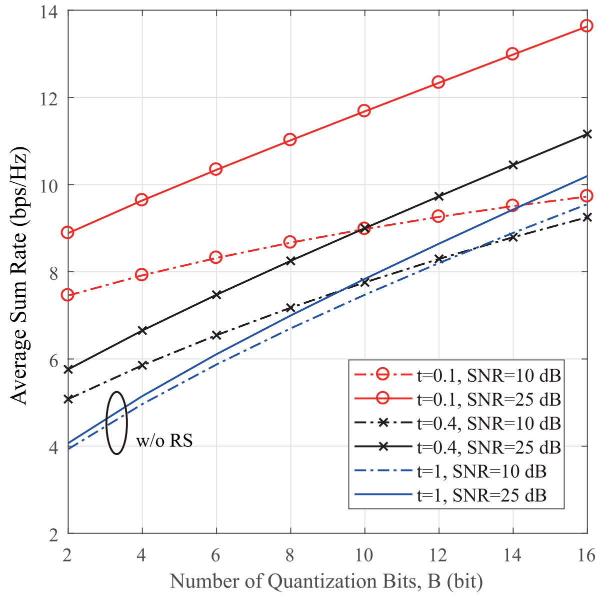

FIGURE 3. Average sum rate versus B with SNR = 10dB or SNR = 25dB.

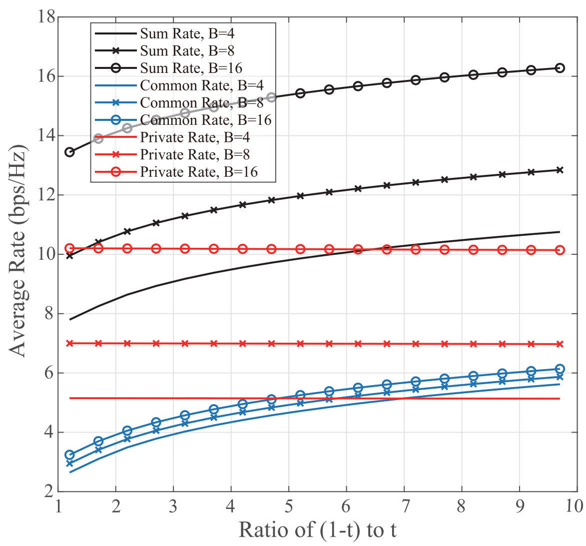

FIGURE 4. Average sum rate versus t with SNR = 30dB.

sum rate is an increasing function of SNR and tends to flatten as SNR increases. This is because in the high-SNR regime, the system is interference-limited, the residual interference from quantization limits the average sum rate growth, which is also verified by the asymptotic private and common rate expressions in (67b) and (68b) independent of Υ. Then, as the number of quantization bits increases, the average sum rate grows due to the improvement of CSIT quality. Next, compared with conventional IA, RS can elevate the average sum rate, even for the worse CSIT quality. Because RS can transmit one more common stream than the conventional schemes and obtain extra multiplexing gain via power allocation. At last, signal alignment can improve the performance of RS dramatically. Although signal alignment results in extra alignment error, the alignment between common and private signals is beneficial to SIC detecting process, which implies that the gain from signal alignment can counteract the impact of alignment error. From the simulation results and analysis above, we can draw a conclusion that RS with lower CSIT error sensibility is more robust than IA; meanwhile alignment can further improve the SIC decoding accuracy, and thus increase the average sum rate for RS.

Fig. 3 to 5 illustrate the relationships between average sum rate and number of quantization bits B along with power allocation factor t under signal alignment, respectively.

In Fig. 3, it is clear that the average sum rate is an increasing function of B. The gain obtained by RS over SIA decreases as B increases under lower SNR (SNR = 10dB); the gain doesn't degrade significantly with more quantization bits under higher SNR (SNR = 25dB). It illustrates that under lower SNR, if CSIT quality is sufficiently high, IA and RS can reach the comparable average sum rate; under higher SNR, to get the same performance, RS needs much less quantization bits than IA does. We can see that whatever the CSIT quality is, RS can achieve better performance of sum rate than IA, which also proves that RS is a robust transmission scheme.

In Fig. 4, the average common, private and sum rate are illustrated versus the ratio of $(1 - t)$ to t that is the ratio of power allocated to common and private parts. To guarantee the order of SIC decoding (first decoding the common part and then the private one), it makes sense that $(1 - t)/t > 1$. In the figure, we can observe that as $(1 - t)/t$ increases the common rate increase while the private rate decreases slightly. Since the increments brought by the common part are much more than the decrements from private one, the combination result is that the average sum rate grows with increasing $(1-t)/t$. In Fig. 5, the combining effects of B and t

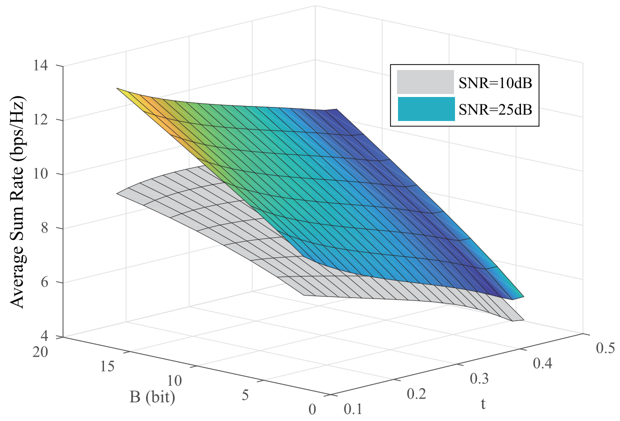

FIGURE 5. Average sum rate versus B and t with SNR = 10dB or SNR = 25dB.

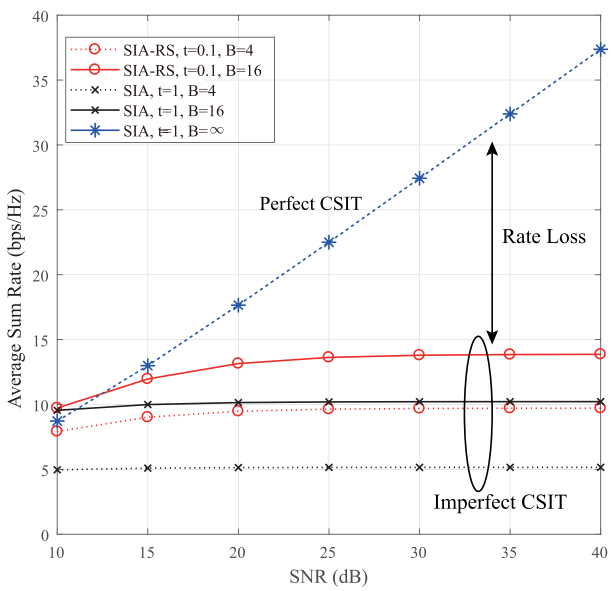

FIGURE 6. Average sum rate loss versus SNR with or without RS under $B = 4$ or $B = 16$.

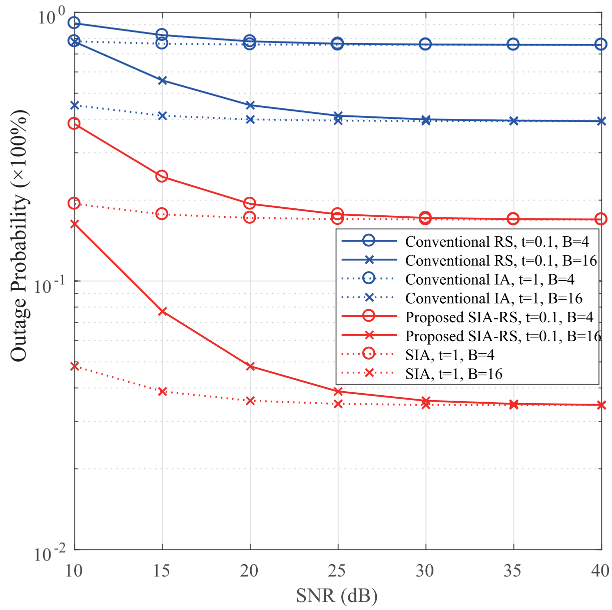

FIGURE 7. Comparison of outage probability versus SNR among various schemes with $B = 4$ or $B = 16$.

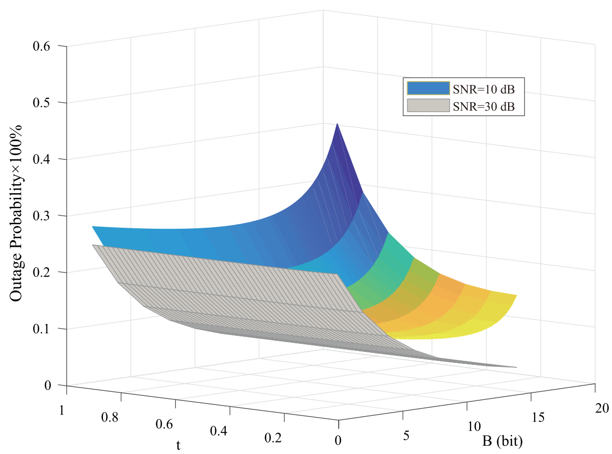

FIGURE 8. Outage probability versus B and t with SNR = 10dB or SNR = 30dB.

on average sum rate under SNR = 10dB and SNR = 25dB is shown.

Fig. 6 verifies the results about the impact of quantization error on average sum rate loss in Section IV-A. Under lower SNR, the impact of quantization error on average sum rate can be ignored. As SNR increases, the sum rate under perfect CSIT keeps growing, while the sum rate under imperfect CSIT tends to flatten, which is because the residual interference from quantization error limits the performance enhancement.

C. OUTAGE PROBABILITY

Fig. 7 depicts the relationships between outage probability and SNR under the different schemes. Outage probability is a decreasing function of SNR. In contrast with the performance of average sum rate, RS doesn't bring out lower outage probability, even worse than IA schemes. This is because the SIC decoding process of RS increases the outage probability significantly. On the other hand, signal alignment can improve the outage probability, which verifies that signal alignment is beneficial to the successful SIC decoding.

Fig. 8 presents the impact of B and t on outage probability. The outage probability is a decreasing function of B. For the low SNR, the outage probability declines as t gets larger; for higher SNR, the outage probability tends to a constant, independent of t, which has been proved in Section IV-B.

In Fig. 9, the observations about the outage probability loss given in (71) and its asymptotic version in (72) are further validated. The SIA with $t = 1$ can achieve better performance than RS, and the outage probability tends to flatten in the high-SNR regime.

D. SER

Fig. 10 illustrates how the SER of private and common parts varies with SNR under the different modulation schemes.

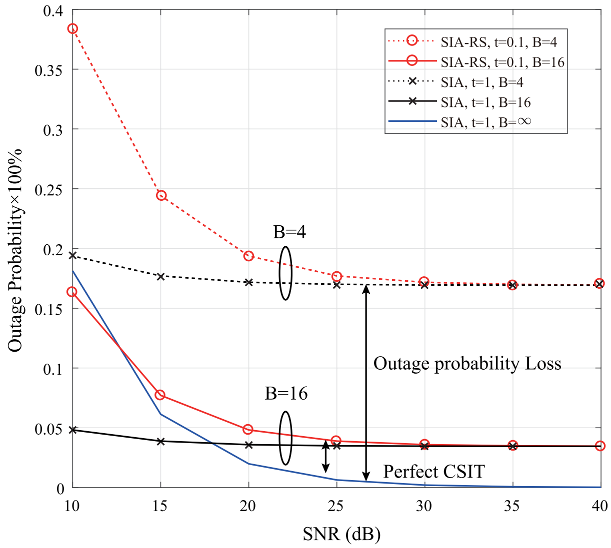

FIGURE 9. Outage probability loss versus SNR with or without RS under $B = 4$ or $B = 16$.

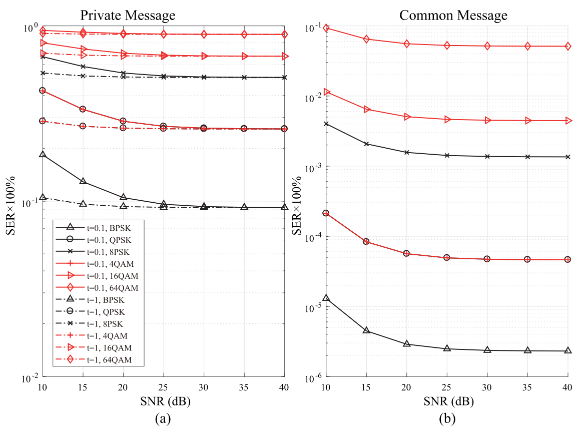

FIGURE 10. Common and private SER versus SNR with or without RS under various modulation schemes.

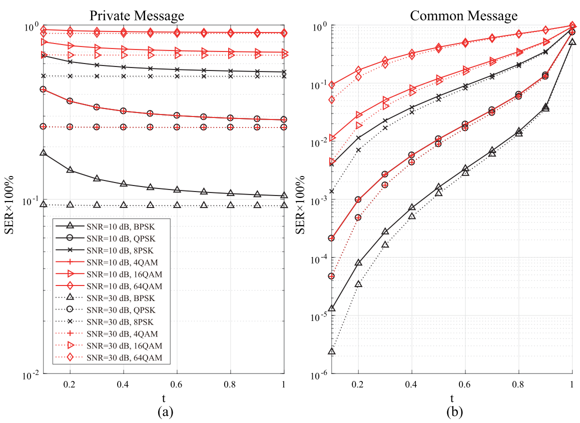

FIGURE 11. Common and private SER versus t with or without RS under various modulation schemes.

The common message's SER is lower since it is allocated more power and thus has larger SINR; the private one has higher SER since its SINR is smaller. So we can get the implication that the suitable modulation schemes for common and private parts can be selected separately. Under a certain threshold of SER, the higher-order modulation schemes, such as 8PSK, 16QAM etc.,can be chosen for common message to improve the efficiency; the lower-order modulation schemes, like BPSK, are suitable for private part to increase accuracy.

In Fig. 11, the relationship between the SER and t is given for private and common parts under the various modulation schemes. As t gets larger, the private SINR increases, and thus the private SER reduces while the common SINR decreasing leads to the higher common SER. In the feasible range of RS, $0 < t < 0.5$, under a certain threshold, the modulation order selected for common message degrades as t increases.

VI. CONCLUSION

In this paper, we proposed a novel transmission scheme named by signal and interference alignment based rate splitting (SIA-RS), and comprehensively analyzed the performance under CSIT quantization error via giving the closed-from expressions of average sum rate, outage probability and SER and their asymptotic versions under the high SNR. Differing from conventional transmission, due to signal alignment and common message, there existed the correlation between key variables. We have applied the nested finite weighted sum of independent and correlated Erlang RVs to approximate the performance expressions.

Through derivation and analysis, the relationship between RS and IA has been revealed. As for the average sum, RS could improve the robustness of conventional transmission effectively since the common message was independent of the CSIT accuracy, which could also bring out extra multiplexing gain. Meanwhile, the simulation results have shown that common and private signal alignment could improve the performance of RS because signal alignment was beneficial to the accuracy enhancement of SIC decoding process. From the results of outage probability, we have seen that RS had worse outage probability than IA schemes due to SIC decoding process; signal alignment could improve the outage probability significantly. We could conclude that IA is more reliable than RS, and alignment can enhance the outage performance of RS. In terms of SER results, a novel RS-based adaptive modulation scheme has been provided, where common and private massages were modulated separately with different schemes, that is, common part employed higher-order modulation for efficiency and private used lower-order for accuracy. Therefore, we have drawn a conclusion that the combination of "spitting" and "alignment" ideas can bring out a robust and reliable transmission.

As the future work, we will further study the method to optimize the value of t of the proposed scheme and compare it with the optimal t of the conventional RS scheme given by [28].

APPENDIX A
PROOF OF PROPOSITION 1

The signal alignment equation in (6) is re-written as

$$\left[\hat{\mathbf{H}}_{k,k}, -\hat{\mathbf{H}}_{k}\right]\begin{bmatrix}\hat{\mathbf{v}}_k^{(p)}\\ \hat{c}_k^{(p)}\hat{\mathbf{v}}^{(c)}\end{bmatrix} = 0 \Rightarrow \begin{bmatrix}\hat{\mathbf{v}}_k^{(p)}\\ \hat{c}_k^{(p)}\hat{\mathbf{v}}^{(c)}\end{bmatrix} = \mathbf{V}_k\mathbf{z}_k, \quad (74)$$

where $\mathbf{V}_k$ is a matrix comprised of $(K+1)N_t - N_r$ left singular vectors of $[\hat{\mathbf{H}}_{k,k}, -\hat{\mathbf{H}}_k]$ that correspond to zero singular value, and $\mathbf{z}_k \in \mathbb{R}^{(K+1)N_t - N_r}$ is a constant vector used to satisfy the power constraint.

Then we have

$$\hat{\mathbf{g}}_{k,k} = \frac{1}{2}\left[\hat{\mathbf{H}}_{k,k}, \hat{\mathbf{H}}_k\right]\begin{bmatrix}\hat{\mathbf{v}}_k^{(p)} \\ \hat{c}_k^{(p)}\hat{\mathbf{v}}^{(c)}\end{bmatrix} = \frac{1}{2}\left[\hat{\mathbf{H}}_{k,k}, \hat{\mathbf{H}}_k\right]\mathbf{V}_k\mathbf{z}_k. \quad (75)$$

According to Proposition 1 in [29], $\hat{\mathbf{g}}_{k,k} \sim \mathcal{CN}(\mathbf{0}, \mathbf{I}_{N_t})$.

Let $\bar{\mathbf{G}}_k = [\hat{\mathbf{g}}_{k,1}, \cdots, \hat{\mathbf{g}}_{k,k-1}, \hat{\mathbf{g}}_{k,k+1}, \cdots, \hat{\mathbf{g}}_{k,K}] \in \mathbb{C}^{N_r \times (K-1)}$, the IA condition in (3) is re-written as

$$\hat{\mathbf{u}}_k^{\mathrm{H}}\bar{\mathbf{G}}_k = 0, \quad (76)$$

which means that $\hat{\mathbf{u}}_k$ is in the nullspace of $\bar{\mathbf{G}}_k^{\mathrm{H}}$. The projection matrix to the column space of $\bar{\mathbf{G}}$ is $\mathbf{\Pi}_{\bar{\mathbf{G}}_k} = \bar{\mathbf{G}}_k(\bar{\mathbf{G}}_k^{\mathrm{H}}\bar{\mathbf{G}}_k)^{-1}\bar{\mathbf{G}}_k^{\mathrm{H}}$, and the orthogonal projection matrix is $\mathbf{\Pi}_{\bar{\mathbb{G}}_k}^{\perp} = \mathbf{I}_{N_r} - \mathbf{\Pi}_{\bar{\mathbb{G}}_k}$. Since $N_r = N_t = K$, $\mathrm{rank}(\mathbf{\Pi}_{\bar{\mathbf{G}}_k}^{\perp}) = 1$. For $\mathbf{\Pi}_{\bar{\mathbf{G}}_k}^{\perp}\hat{\mathbf{u}}_k = \hat{\mathbf{u}}_k$, $\hat{\mathbf{u}}_k$ is the eignvector corresponding to eignvalue 1 of $\mathbf{\Pi}_{\bar{\mathbf{G}}_k}^{\perp}$. And thus we have,

$$|\hat{h}_{k,k}|^2 = \left|\hat{\mathbf{u}}_k^{\mathrm{H}}\hat{\mathbf{g}}_{k,k}\right|^2 = \hat{\mathbf{g}}_{k,k}^{\mathrm{H}}\mathbf{\Pi}_{\bar{\mathbf{G}}_k}^{\perp}\hat{\mathbf{g}}_{k,k}. \quad (77)$$

Since $\hat{\mathbf{g}}_{k,k} \sim \mathcal{CN}(\mathbf{0}, \mathbf{I}_{N_t})$, based on [17], $|\hat{h}_{k,k}|^2$ is exponentially distributed, i.e., $|\hat{h}_{k,k}|^2 \sim \chi^2(2)$.

APPENDIX B
PROOF OF LEMMA 1

$$\begin{aligned}
&\mathbb{E}\left\|\hat{\mathbf{H}}_{k,k}^{-1}\hat{\mathbf{H}}_k\mathbf{v}^{(c)}\right\|^2 \\
&\le \mathbb{E}\left\|\hat{\mathbf{H}}_{k,k}^{-1}\hat{\mathbf{H}}_k\right\|^2\|\mathbf{v}^{(c)}\|^2 \quad (78)\\
&= K\mathbb{E}\left\|\left[\hat{\mathbf{H}}_{k,k}^{-1}\hat{\mathbf{H}}_{k,1}, \ldots, \hat{\mathbf{H}}_{k,k}^{-1}\hat{\mathbf{H}}_{k,k-1}, \mathbf{I}_{N_t},\right.\right. \\
&\qquad \left.\left.\hat{\mathbf{H}}_{k,k}^{-1}\hat{\mathbf{H}}_{k,k+1}, \ldots, \hat{\mathbf{H}}_{k,k}^{-1}\hat{\mathbf{H}}_{k,K}\right]\right\|^2 \\
&= K\mathrm{tr}\left(\mathbf{I}_{N_t}\right) + \sum_{j\in\mathcal{K}\setminus\{k\}}\mathbb{E}\left\{\mathrm{tr}(\hat{\mathbf{H}}_{k,k}^{-1}\hat{\mathbf{H}}_{k,j}\hat{\mathbf{H}}_{k,j}^{\mathrm{H}}\hat{\mathbf{H}}_{k,k}^{-H})\right\} \\
&= KN_t, \quad (79)
\end{aligned}$$

where (78) is from Cauchy-Schwartz inequality. Since $\hat{\mathbf{H}}_{k,k}$ and $\mathbf{H}_{k,j}$ with $j \ne k$ are uncorrelated, $\mathbb{E}\left\{\mathrm{tr}(\hat{\mathbf{H}}_{k,k}^{-1}\hat{\mathbf{H}}_{k,j}\hat{\mathbf{H}}_{k,j}^{\mathrm{H}}\hat{\mathbf{H}}_{k,k}^{-H})\right\} = 0$

APPENDIX C
PROOF OF LEMMA 4

The proof is referred to [30]. Let $A_1 \sim \mathrm{Exp}(\lambda_1)$ and $A_2 \sim \mathrm{Exp}(\lambda_2)$ to be two correlated exponential RVs with lower and upper bounds of the correlation coefficient $\rho_{\min}$ and $\rho_{\max}$, corresponding to counter-monotonic and co-monotonic A_1 and A_2, respectively. The CDF and quantile function of exponential distribution are $F(x) = 1-\exp(-\lambda x)$ and $F^{-1}(q)(-\lambda^{-1}\ln(1-q))$, respectively. Let $U \sim \mathrm{U}(0, 1)$ to be uniformly distributed RV, and thus $1 - U$ is also uniformly distributed.

Let $A_1 = -\lambda_1^{-1}\ln(1-U)$ and $A_2 = -\lambda_2^{-1}\ln(U)$ to be exponentially distributed RVs with parameters λ_1 and λ_2, respectively. $h_1(x) \triangleq -\lambda_1^{-1}\ln(1-x)$ and $h_2(x) \triangleq -\lambda_1^{-1}\ln(x)$ are monotonically increasing and decreasing, respectively. And we have

$$\begin{aligned}
\mathbb{E}\{A_1A_2\} &= \frac{1}{\lambda}\mathbb{E}\{\ln(1-U)\ln(U)\} \\
&= \frac{1}{\lambda_1\lambda_2}\int_0^1 \ln(1-u)\ln(u)f_U(u)du \\
&= \frac{1}{\lambda_1\lambda_2}\left(2 - \frac{\pi^2}{6}\right), \quad (80)
\end{aligned}$$

where $f_U(u) = 1$ is the density function of the standard uniform distribution, (80) is derived from [24, (4.221.1)]. Then, the correlation coefficient between A_1 and A_2 is given by

$$\begin{aligned}
\rho_{\min} = \mathrm{corr}(A_1, A_2) &= \frac{\mathbb{E}\{A_1A_2\} - (\lambda_1\lambda_2)^{-1}}{(\lambda_1\lambda_2)^{-1}} \\
&= 1 - \pi^2/6 \approx -0.645. \quad (81)
\end{aligned}$$

Similarly, as for $\rho_{\max}$, let $A_1 = -\lambda_1^{-1}\ln(1-U)$ and $A_1 = -\lambda_2^{-1}\ln(1-U)$, where $g_i(x) = -\lambda_i^{-1}\ln(1-x)$ for $i = \{1, 2\}$ are both monotonically increasing. So

$$\begin{aligned}
\mathbb{E}\{A_1A_2\} &= \frac{1}{\lambda_1\lambda_2}\int_0^1 \ln(1-u)\ln(u)f_U(u)du \\
&= \frac{2}{\lambda_1\lambda_2}. \quad (82)
\end{aligned}$$

Then, the correlation coefficient between A_1 and A_2 is given by

$$\rho_{\max} = \mathrm{corr}(A_1, A_2) = \frac{\mathbb{E}\{A_1A_2\} - (\lambda_1\lambda_2)^{-1}}{(\lambda_1\lambda_2)^{-1}} = 1. \quad (83)$$

REFERENCES

[1] G. Zheng, I. Krikidis, C. Masouros, S. Timotheou, D.-A. Toumpakaris, and Z. Ding, "Rethinking the role of interference in wireless networks," *IEEE Commun. Mag.*, vol. 52, no. 11, pp. 152–158, Nov. 2014.
[2] V. R. Cadambe and S. A. Jafar, "Interference alignment and degrees of freedom of the K-user interference channel," *IEEE Trans. Inf. Theory*, vol. 54, no. 8, pp. 3425–3441, Aug. 2008.
[3] Z. Li, Y. Bai, K. G. Shin, Z. Yan, and H. Li, "Inside-out precoding to manage multiple interferences from the same source," *IEEE Trans. Veh. Technol.*, vol. 69, no. 7, pp. 7583–7595, Jul. 2020.
[4] T. Han and K. Kobayashi, "A new achievable rate region for the interference channel," *IEEE Trans. Inf. Theory*, vol. IT-27, no. 1, pp. 49–60, Jan. 1981.
[5] S. Yang, M. Kobayashi, D. Gesbert, and X. Yi, "Degrees of freedom of time correlated MISO broadcast channel with delayed CSIT," *IEEE Trans. Inf. Theory*, vol. 59, no. 1, pp. 315–328, Jan. 2013.
[6] A. Gholami Davoodi and S. A. Jafar, "Generalized degrees of freedom of the symmetric K user interference channel under finite precision CSIT," *IEEE Trans. Inf. Theory*, vol. 63, no. 10, pp. 6561–6572, Oct. 2017.
[7] B. Clerckx, H. Joudeh, C. Hao, M. Dai, and B. Rassouli, "Rate splitting for MIMO wireless networks: A promising PHY-layer strategy for LTE evolution," *IEEE Commun. Mag.*, vol. 54, no. 5, pp. 98–105, May 2016.
[8] C. Hao, Y. Wu, and B. Clerckx, "Rate analysis of two-receiver MISO broadcast channel with finite rate feedback: A rate-splitting approach," *IEEE Trans. Commun.*, vol. 63, no. 9, pp. 3232–3246, Sep. 2015.

[9] H. Joudeh and B. Clerckx, "Sum-rate maximization for linearly precoded downlink multiuser MISO systems with partial CSIT: A rate-splitting approach," *IEEE Trans. Commun.*, vol. 64, no. 11, pp. 4847–4861, Nov. 2016.

[10] H. Joudeh and B. Clerckx, "Rate-splitting for max-min fair multigroup multicast beamforming in overloaded systems," *IEEE Trans. Wireless Commun.*, vol. 16, no. 11, pp. 7276–7289, Nov. 2017.

[11] M. Dai, B. Clerckx, D. Gesbert, and G. Caire, "A rate splitting strategy for massive MIMO with imperfect CSIT," *IEEE Trans. Wireless Commun.*, vol. 15, no. 7, pp. 4611–4624, Jul. 2016.

[12] Y. Mao, B. Clerckx, and V. O. K. Li, "Rate-splitting multiple access for downlink communication systems: Bridging, generalizing, and outperforming SDMA and NOMA," *EURASIP J. Wireless Commun. Netw.*, vol. 2018, no. 1, p. 133, Dec. 2018.

[13] C. Hao and B. Clerckx, "MISO networks with imperfect CSIT: A topological rate-splitting approach," *IEEE Trans. Commun.*, vol. 65, no. 5, pp. 2164–2179, May 2017.

[14] Y. Mao, B. Clerckx, and V. O. K. Li, "Rate-Splitting Multiple Access for Coordinated Multi-Point Joint Transmission," in *Proc. IEEE Int. Conf. Commun. Workshops (ICC Workshops)*, May 2019, pp. 1–6.

[15] M. Gil Kang and W. Choi, "Interference alignment with rate splitting in a three-user interference channel with a cognitive transmitter," in *Proc. IEEE Global Commun. Conf. (GLOBECOM)*, Dec. 2012, pp. 2203–2208.

[16] J. Lindblom, E. Karipidis, and E. G. Larsson, "Efficient computation of Pareto optimal beamforming vectors for the MISO interference channel with successive interference cancellation," *IEEE Trans. Signal Process.*, vol. 61, no. 19, pp. 4782–4795, Oct. 2013.

[17] Z. Ding, R. Schober, and H. V. Poor, "A general MIMO framework for NOMA downlink and uplink transmission based on signal alignment," *IEEE Trans. Wireless Commun.*, vol. 15, no. 6, pp. 4438–4454, Jun. 2016.

[18] C. Suh and D. Tse, "Interference alignment for cellular networks," in *Proc. 46th Annu. Allerton Conf. Commun., Control, Comput.*, Sep. 2008, pp. 1037–1044.

[19] N. Jindal, "MIMO broadcast channels with finite-rate feedback," *IEEE Trans. Inf. Theory*, vol. 52, no. 11, pp. 5045–5060, Nov. 2006.

[20] T. Yoo, N. Jindal, and A. Goldsmith, "Multi-antenna downlink channels with limited feedback and user selection," *IEEE J. Sel. Areas Commun.*, vol. 25, no. 7, pp. 1478–1491, Sep. 2007.

[21] J. Zhang, R. W. Heath, M. Kountouris, and J. G. Andrews, "Mode switching for the multi-antenna broadcast channel based on delay and channel quantization," *EURASIP J. Adv. Signal Process.*, vol. 2009, no. 1, pp. 1–15, Dec. 2009.

[22] X. Chen and C. Yuen, "On interference alignment with imperfect CSI: Characterizations of outage probability, ergodic rate and SER," *IEEE Trans. Veh. Technol.*, vol. 65, no. 1, pp. 47–58, Jan. 2016.

[23] G. K. Karagiannidis, N. C. Sagias, and T. A. Tsiftsis, "Closed-form statistics for the sum of squared Nakagami-m variates and its applications," *IEEE Trans. Commun.*, vol. 54, no. 8, pp. 1353–1359, Aug. 2006.

[24] I. Gradshteyn and I. Ryzhik. (2007). *Table of Integrals, Series, and Products*. [Online]. Available: http://fisica.ciens.ucv.ve/~svincenz/TISPISGIMR.pdf

[25] M. Deghel, E. Bastug, M. Assaad, and M. Debbah, "On the benefits of edge caching for MIMO interference alignment," in *Proc. IEEE 16th Int. Workshop Signal Process. Adv. Wireless Commun. (SPAWC)*, Jun. 2015, pp. 655–659.

[26] M. Z. Win, G. Chrisikos, and J. H. Winters, "MRC performance for M-ary modulation in arbitrarily correlated nakagami fading channels," *IEEE Commun. Lett.*, vol. 4, no. 10, pp. 301–303, Oct. 2000.

[27] M. R. Leadbetter, G. Lindgren, and H. Rootzen, *Extremes and Related Properties of Random Sequences and Processes* (Springer Series in Statistics). New York, NY, USA: Springer, 2012.

[28] A. Salem, C. Masouros, and B. Clerckx, "Rate splitting with finite constellations: The benefits of interference exploitation vs suppression," 2019, *arXiv:1907.08457*. [Online]. Available: https://arxiv.org/abs/1907.08457

[29] Z. Ding, T. Wang, M. Peng, W. Wang, and K. K. Leung, "On the design of network coding for multiple two-way relaying channels," *IEEE Trans. Wireless Commun.*, vol. 10, no. 6, pp. 1820–1832, Jun. 2011.

[30] (Apr. 13, 2017). *Attainable Correlations for Exponential Random Variables*. [Online]. Available: https://stats.stackexchange.com/q/66776 and https://stats.stackexchange.com/users/27403/quantibex

XIN SU (Member, IEEE) received the bachelor's and Ph.D. degrees in information and communication engineering from the Beijing University of Posts and Telecommunications, Beijing, China, in 2008 and 2019, respectively. In 2020, she joined the Future Mobile Technology Laboratory, China Mobile Research Institute. Her research interests include multicell cooperation, intelligent reflection surface, virtual multi-input multi-output, and advanced signal processing.

YIFEI YUAN (Senior Member, IEEE) received the B.S. and M.S. degrees in precision instruments from Tsinghua University, Beijing, China, in 1993 and 1996, respectively, and the Ph.D. degree in electrical and computer engineering from Carnegie Mellon University, Pittsburgh, PA, USA, in 2000.

He joined Lucent Technologies, in 2000, as a Technical Staff Member, working on key technologies for 3G. In 2008, he joined ZTE, as a Chief Engineer of wireless standards, responsible for research and standardization of 4G and 5G. He joined the China Mobile Research Institute, Beijing, as a Chief Expert, in 2020, responsible for 6G. He was admitted to the Thousand Talent Plan Program of China, in 2010. He has extensive publications, including three books on 4G LTE and four books on 5G. He holds over 50 granted patents. His research interests include multi-input multi-output, channel coding, non-orthogonal multiple access (NOMA), resource scheduling, and the IoT. He received the IEEE Asian-Pacific Best Paper Award, in 2018. He serves as the Chief Editor for *Hans Journal of Wireless Communications*. He also serves as an Editor for the IEEE COMMUNICATIONS LETTERS and *China Communications*.

QIXING WANG received the B.S., M.S., and Ph.D. degrees in information and communication engineering from the Beijing University of Posts and Telecommunications, Beijing, China, in 2002, 2005, and 2008, respectively.

From 2008 to 2019, he was with the Department of Wireless and Terminal Technology, China Mobile Research Institute, working on the research and standardization of 4G and 5G, where he joined the Future Mobile Technology Laboratory, in 2020, as a Principal Member of technical staff responsible for 6G. His research interests include virtual multi-input multi-output, holographic multi-input multi-output, and 4D-multi-input multi-output.